ON SEISMIC WAVES.

(Second Paper.)

By

B. Gutenberg

Balch Graduate School of the Geological Sciences, California Institute of Technology, Pasadena

Contribution No. 169

and

C. F. Richter

Carnegie Institution of Washington, Seismological Research, Pasadena (California).

(With 16 figures.)

Contents.

I. Introductory 282
II. Seismograms used 282
III. Statistical survey of periods 288
IV. Compressions and dilatations 290
V. Theoretical considerations on amplitudes, travel times, velocities and their relation 298
VI. Theory of the amplitude ratio PP/P. Effect of crustal structure 305
VII. Observations of PP/P 308
A. Continental reflections p. 308. — B. Pacific reflections p. 313. — C. Atlantic reflections p. 318. — D. Reflections in the Indian Ocean p. 318. — E. Reflections in the Arctic Basin p. 320. — F. Special and exceptional cases p. 324.
VIII. Other amplitude ratios 325
A. PPP/P p. 325. — B. PP/P' p. 325. — C. Amplitudes of SS p. 325. — D. Amplitudes of PS, PPS and $SKSP$ p. 326.
IX. Appearance of normal seismograms at various distances 326
X. P and S at short distances. The problem of discontinuities in the mantle of the earth 332
XI. Calculations for velocities of P and S at various depths in the mantle 344
XII. Velocity distribution within the core 352
XIII. Calculated and observed travel times; additional data 357
XIV. Poisson's Ratio 358
References 358

Zusammenfassung: Als Material für die vorliegende Veröffentlichung wurden die in der ersten Arbeit[1]) sowie die in den Tabellen 1 und 2 angegebenen Seismogramme benutzt.

Während die Perioden der Vorläufer in Herdnähe mit wachsender Entfernung zunehmen, ist dies bei Herdentfernungen über 2000 km im allgemeinen nicht mehr der Fall. Die Tabellen 3 und 4 geben vorherrschende Perioden in verschiedenen Phasen für größere Herdentfernungen.

Erdbeben aus bestimmten Epizentralgebieten zeigen in Pasadena fast stets den gleichen Anfang (Kompression oder Dilatation), und zwar meist gleichartig in normalen Beben und solchen mit anormal tiefen Herden (Tabelle 5). Es läßt dies auf gleichartigen Mechanismus schließen. Ähnliches wurde früher für normale Beben an anderen Stationen gefunden. In Alaska-Beben überwiegen normalerweise fast an allen Stationen der Erde Kompressionen im Anfang von P, so daß in diesen Beben Vertikalbewegungen vorzuherrschen scheinen. Theoretisch sollte PP umgekehrt beginnen wie P, PcP in Herddistanzen zwischen etwa 20° und 75° gleichsinnig. Letzteres wird durch Beobachtungen bestätigt (Fig. 2). Das Verhalten von PcP in kleinen Herdentfernungen und die Amplituden von PcP hängen von dem Verhältnis der Dichten an der Kerngrenze ab. Die Amplitudenbeobachtungen sprechen dafür, daß die Dichte im Kern merklich größer ist als im Mantel an der Kerngrenze.

Um die Amplitudenbeobachtungen besser zur Diskussion der Wellengeschwindigkeit im Erdinnern verwenden zu können, wird das allgemeine Verhalten von Laufzeitkurven, deren Ableitungen sowie der Zusammenhang dieser Werte mit den Amplituden und der Wellengeschwindigkeit in der Tiefe eingehend diskutiert. Die Beziehungen (18) bis (20) geben die wichtigsten Ergebnisse dieser Betrachtungen. Die Theorie zeigt weiter, daß das Amplitudenverhältnis PP/P wesentlich von der Wellengeschwindigkeit an der Reflexionsstelle abhängt. PP sollte im allgemeinen bei Reflexion am „Sima" schwächer sein als bei Reflexion am Kontinentalboden. Der maximale Unterschied sollte in etwa 45° Herdentfernung auftreten, wo PP im ersten Falle nur etwa $^1/_4$ der Amplituden besitzen sollte als im zweiten. Die Beobachtungen (vgl. Fig. 6 und 7) bestätigen dies. Sie zeigen weiter, daß PP-Wellen, die in einem Gebiet südlich der Galapagos-Inseln reflektiert wurden, kontinentale Amplituden zeigen. Solche treten weiterhin überall bei Reflexionen im Atlantischen und Indischen Ozean auf, so daß wir in diesen Fällen eine kontinentale Kruste annehmen müssen, deren Dicke nicht klein gegenüber der Wellenlänge von etwa 20 km sein kann. Im Nordpolarbecken zeigen die meisten Reflexionen pazifischen Charakter, während Reflexionen in Nordgrönland und dem anschließenden Schelf bei den gleichen Beben kontinentalen Charakter besitzen. Demnach scheint im Polarbecken stellenweise die kontinentale Kruste ganz zu fehlen oder mindestens sehr dünn zu sein. In einer Reihe von Fällen, z. B. an den Westküsten von Mexiko und Kanada, ist es möglich, auf diesem Wege die Grenze der Kontinentalschollen festzulegen. Messungen von PPP-Amplituden bestätigen die Ergebnisse, die aus PP/P abgeleitet wurden. Das Verhältnis PP/P' zeigt die Wirkung des Brennpunktes von P'. Die großen Amplituden von PS und PPS entsprechen der Theorie.

Das Aussehen der Seismogramme, besonders der für die verschiedenen Herdentfernungen charakteristischen Phasen, wird besprochen und insbesondere das Verhalten von P und S in Seismogrammen aus kleinen Herdentfernungen diskutiert. Die scheinbare Fortpflanzungsgeschwindigkeit von P wird aus Registrierungen der gleichen Beben an Stationspaaren, die etwa 2° voneinander entfernt sind, punktweise gefunden (Fig. 13). Das Ergebnis spricht für eine im Mantel von rund 100 km ab stetig mit der Tiefe anwachsende Wellengeschwindigkeit. Das plötzliche Anwachsen der Amplituden von P in einer Herdentfernung von etwa 13°, die kräftigen P-Wellen in allen folgenden Distanzen bis über 30°, das entsprechende Verhalten von PP und PPP in der doppelten bzw. dreifachen Entfernung widerspricht der Annahme, daß in diesem Entfernungsbereich Wellen auftauchen, die eine Unstetigkeitsfläche unterhalb einer Tiefe von 50 km passiert haben.

Endlich werden die Wellengeschwindigkeiten (Fig. 16) und die Poissonsche Konstante im Erdinnern (Tabelle 27) berechnet. Die Laufzeiten, die sich für die beobachteten Wellen unter Zugrundelegung der Kurven in Fig. 16 ergeben, stimmen gut mit den Beobachtungen überein. Die Herdentfernungen der Brennpunkte von Wellen durch den Erdkern ergeben sich richtig, dagegen werden alle derartigen Wellen an den Brennpunkten etwas früher beobachtet, als berechnet wird. Die einzige Unstetigkeitsfläche erster Ordnung im Erdinnern, von den obersten 100 km abgesehen, ist die Oberfläche des Erdkerns, die sich erneut in rund 2900 km Tiefe ergibt.

I. Introductory.

In a first paper under the present title[1]) the authors have presented a body of data on travel times. The present paper contains the corresponding data on amplitudes, periods, velocities, etc., for bodily waves. It is intended to present data on surface waves in a third paper.

II. Seismograms used.

In what here follows we have used the seismograms and reports listed in the first paper, with additional seismograms of recent shocks at Pasadena, its auxiliary stations, and Huancayo (Table 1). To further supplement the data in certain ranges of distance, and in order to study certain wave-paths chosen for the information they might yield as to the crustal structure of the earth, requests for loan of original seismograms or copies were sent to selected stations. As on previous occasions, the response to these requests has been highly satisfactory. We wish to express our deep indebtedness to the directors of the various stations who have made these records available to us. A list of the seismograms used appears in Table 2, except for a few cases which are listed in the last column of Table 1.

Serial numbers have been attached to the various shocks studied.

Table 1.

No.	Date of shock	Origin time	Region	Distance in degrees from*) Pa.	Hu.	other stations
109	1931 Oct. 1	$11^h\ 46^m$ ca.	Lower California	5		
110	1932 July 7	16 15 36^s	Gulf of California	7		Tinemaha 9°
111	1932 July 12	19 24 01	Gulf of California	11 ½		
112	1931 Jan. 2	09 48 56	Off Mexico	18 ½		
113	1933 April 9	03 58 08	Off Mexico	19¾		See table 15
114	1933 April 9	21 03 19	Off Mexico	19¾		
115	1933 July 22	20 55 10	Aleutian Is.	40 ½	102	
116	1931 July 20	08 30 20	Near Samoa	71		
117	1933 July 24	18 55 38	Near Samoa	71		
118	1933 Sept. 9	21 20 03	New Hebrides	84	112	
119	1934 March 5	11 46 16	New Zealand	96	94 ½	
120	1927 May 22	22 32.6	Kansu	99		
121	1933 Nov. 19	03 11 18	New Hebrides	87	112	
122	1933 Dec. 2	20 04 57	S. of Falkland Is.	102	45	
123	1933 Dec. 12	14 11 12	Bismarck Is.	92	129 ½	
124	1933 Dec. 13	21 23 39	Mexico	20	40 ½	See table 15
125	1933 Dec. 19	17 48 25	Baffin Bay	46		
126	1934 Jan. 28	19 10 04	Mexico	24	38	See table 15
127	1934 Jan. 31	10 06 32	SW. of Samoa	72	96	Mt. Wilson 72°
128	1934 Feb. 3	14 33 05	Bismarck Is.	94	130	
129	1934 Feb. 24	06 23 37	Marianne Is.	84 ½	139	
130	1934 March 4	06 55 06	New Hebrides	86		
131	1934 March 13	13 11 50	Solomon Is.	86 ½	116	
132	1934 March 24	12 04 26	Solomon Is.	87¾	119	

*) Pa. = Pasadena. Hu. = Huancayo (Peru).

Table 1 (continued).

No.	Date of shock	Origin time	Region	Distance in degrees from*) Pa.	Hu.	other stations
133	1934 April 15	22 15 08^s	Off Philippines	106	157	
134	1934 May 4	04 36 02	Alaska	33 ½	92	See table 15
135	1934 May 13	13 11 50	Bismarck Is.	92		
136	1934 July 28	21 36 55	Alaska	34 ½	95	
137	1934 June 18	09 13 44	Alaska	34		
138	1934 May 14	22 12 46	Alaska	33		Tinemaha 30 ½
139	1934 May 19	10 47 34	Guatemala	31	30 ½	Tinemaha 33 ½
140	1934 July 18	01 36 17	Panama	42	21	
141	1934 July 21	10 39 00	Panama	42	21	
142	1934 Sept. 15	06 56 59	Mexico	17 ½	43 ½	See table 15
143	1934 June 2	13 42 33	Iceland	63	87	
144	1934 Aug. 31	05 02 44	Baffin Bay	46	85	
145	1934 June 9	13 58 43	Bismarck Is.	95	133 ½	
146	1934 June 13	22 10 23	Baluchistan	117		
147	1934 July 18	19 40 18	Santa Cruz Is.	84 ½	114	
148	1934 July 21	06 18 13	Santa Cruz Is.	84 ½	114	
149	1934 Aug. 7	03 40 07	Santa Cruz Is.	84 ½		
150	1934 Oct. 26	17 11 02	S. of Japan	89		
151	1932 Oct. 16	12 08 00	Alaska	35 ½		
152	1934 Nov. 5	23 02 22	Aleutian Is.	44	105	Berkeley 39 ½
153	1934 Dec. 3	02 38 20	Honduras	34	28 ½	
154	1934 Nov. 30	02 05 19	Mexico	18 ½	43	See table 15
155	1928 March 22	04 16 59	Mexico			
156	1932 Dec. 21	10 10 11	Nevada		64 ¾	
157	1934 March 12	19 20 13	Utah		64	
158	1934 March 12	15 02 42	Utah		64	
159	1933 May 8	10 33 40	Mexico		38 ½	
160	1933 Jan. 27	22 36 40	Near Samoa		93	

161	1933 Jan. 7	$04^h\ 06^m\ 32^s$	Off northern Japan		136		
162	1933 Jan. 4	01 24 35	Bonin Is.		140		
163	1933 Jan. 4	03 59 28	Alaska		91½		
164	1932 Dec. 31	06 30 47	Off Zululand		100½		
165	1933 May 6	05 33.5	Off Panama		19½		
166	1933 April 19	01 45 44	S. Pacific	87	52		
167	1933 July 21	20 06 47	S. Atlantic		58		
168	1933 Nov. 21	23 48 32	Panama		22		
169	1931 Jan. 15	01 50 36	Mexico	27		Honolulu 58°	
170	1932 June 2	10 36.5	Mexico			Honolulu 50°	
171	1932 July 25	09 12.2	Mexico			Honolulu 50°	
172	1932 June 22	12 59.3	Mexico			Honolulu 50°	
173	1934 Dec. 17	15 52 32	Bismarck Is.		134		
174	1934 Dec. 15	01 57 32	Tibet		156		
175	1934 Dec. 30	13 52 04	Lower California		58		
176	1934 Dec. 31	18 45 42	Lower California		58		
177	1934 Dec. 22	14 29½ ±	Nicaragua		24½		
178	1934 Sept. 26	07 27 18	Central Atlantic		45		
179	1934 May 5	14 32.5	New Zealand		95		
180	1934 March 7	22 41 44	NW. Nicaragua	34½	27½		
181	1934 Feb. 28	14 21 23	Bismarck Is.		130		
182	1934 April 9	15 29 24	SE. Pacific	73	32½		
183	1934 Feb. 20	03 18 44	W. of Galapagos Is.	41½	31½		
184	1934 March 15	10 46.7	New Zealand		95		
185	1927 Oct. 24	15 59 51	Alaska[2])				

*) Pa. = Pasadena. Hu. = Huancayo (Peru).

Table 1 (continued).

No.	Date of shock	Origin time	Region	Distance in degrees from*) Pa.	Hu.	other stations
133	1934 April 15	22 15 08^s	Off Philippines	106	157	
134	1934 May 4	04 36 02	Alaska	33 ½	92	See table 15
135	1934 May 13	13 11 50	Bismarck Is.	92		
136	1934 July 28	21 36 55	Alaska	34 ½	95	
137	1934 June 18	09 13 44	Alaska	34		
138	1934 May 14	22 12 46	Alaska	33		Tinemaha 30 ½
139	1934 May 19	10 47 34	Guatemala	31	30 ½	Tinemaha 33 ½
140	1934 July 18	01 36 17	Panama	42	21	
141	1934 July 21	10 39 00	Panama	42	21	
142	1934 Sept. 15	06 56 59	Mexico	17 ½	43 ½	See table 15
143	1934 June 2	13 42 33	Iceland	63	87	
144	1934 Aug. 31	05 02 44	Baffin Bay	46	85	
145	1934 June 9	13 58 43	Bismarck Is.	95	133 ½	
146	1934 June 13	22 10 23	Baluchistan	117		
147	1934 July 18	19 40 18	Santa Cruz Is.	84 ½	114	
148	1934 July 21	06 18 13	Santa Cruz Is.	84 ½	114	
149	1934 Aug. 7	03 40 07	Santa Cruz Is.	84 ½		
150	1934 Oct. 26	17 11 02	S. of Japan	89		
151	1932 Oct. 16	12 08 00	Alaska	35 ½		
152	1934 Nov. 5	23 02 22	Aleutian Is.	44	105	Berkeley 39 ½
153	1934 Dec. 3	02 38 20	Honduras	34	28 ½	
154	1934 Nov. 30	02 05 19	Mexico	18 ½	43	See table 15
155	1928 March 22	04 16 59	Mexico			
156	1932 Dec. 21	10 10 11	Nevada		64 ¾	
157	1934 March 12	19 20 13	Utah		64	
158	1934 March 12	15 02 42	Utah		64	
159	1933 May 8	10 33 40	Mexico		38 ½	
160	1933 Jan. 27	22 36 40	Near Samoa		93	

161	1933 Jan. 7	$04^h\ 06^m\ 32^s$	Off northern Japan		136		
162	1933 Jan. 4	01 24 35	Bonin Is.		140		
163	1933 Jan. 4	03 59 28	Alaska		91½		
164	1932 Dec. 31	06 30 47	Off Zululand		100½		
165	1933 May 6	05 33.5	Off Panama		19½		
166	1933 April 19	01 45 44	S. Pacific	87	52		
167	1933 July 21	20 06 47	S. Atlantic		58		
168	1933 Nov. 21	23 48 32	Panama		22		
169	1931 Jan. 15	01 50 36	Mexico	27		Honolulu 58°	
170	1932 June 2	10 36.5	Mexico			Honolulu 50°	
171	1932 July 25	09 12.2	Mexico			Honolulu 50°	
172	1932 June 22	12 59.3	Mexico			Honolulu 50°	
173	1934 Dec. 17	15 52 32	Bismarck Is.		134		
174	1934 Dec. 15	01 57 32	Tibet		156		
175	1934 Dec. 30	13 52 04	Lower California		58		
176	1934 Dec. 31	18 45 42	Lower California		58		
177	1934 Dec. 22	14 29½ ±	Nicaragua		24½		
178	1934 Sept. 26	07 27 18	Central Atlantic		45		
179	1934 May 5	14 32.5	New Zealand		95		
180	1934 March 7	22 41 44	NW. Nicaragua	34½	27½		
181	1934 Feb. 28	14 21 23	Bismarck Is.		130		
182	1934 April 9	15 29 24	SE. Pacific	73	32½		
183	1934 Feb. 20	03 18 44	W. of Galapagos Is.	41½	31½		
184	1934 March 15	10 46.7	New Zealand		95		
185	1927 Oct. 24	15 59 51	Alaska[2])				

*) Pa. = Pasadena. Hu. = Huancayo (Peru).

Table 2.

No.	Region	Distance in degrees from*)																	
1	Texas	Ch	22¼	Si	34	Ci	17	Ot	26½	Sa	21	Fl	14	SL	14	Gg	23½		
3	Mexico	Ot	35½	Sa	33½	Si	44	SJ	36	LR	19½	Fl	23¼	SL	23¼	Ho	50½	Gg	30¾
6	Mexico	Ci	28½	Ot	37½	Fl	25	SL	25	Hu	41½								
11	Alaska	Ch	48	Ho	40	Ot	44	Hx	50	LR	44	Fl	42	SL	42	Te	48½		
13	Hawaii	Vi	38																
23	Off New Foundld.	Vi	45																
24	Colombia	Lz	25¼	La	45½	RJ	42½												
25	Ecuador	Lz	18½	La	38	RJ	41	Hu	11										
27	Peru	Lz	15	La	34	RJ	37½												
29	Kamchatka	Be	39½																
32	N. Atlantic	SJ	42½	SS	15½	Iv	8½	Ha	27										
34	W. of Easter I.	Be	64	Vi	75														
35	Centr. Atlantic	SJ	56	Te	66½														
37	Peru	La	24¼																
40	N. Chile	We	93½	Cr	93½	Be	75½	La	18	RJ	25	Hu	10						
42	Centr. Atlantic	SS	60																
44	Japan	Ho	52																
46	East Atlantic	SJ	47	SS	31½														
48	Chile	We	85½																
49	Chile	We	83	Lz	17½	La	12½	RJ	27½										
50	Chile	Lz	19¼	La	12½	RJ	29												
76	Off Africa	Gg	71	Ha	69½														
83	Philippines	We	64																
89	India	Hu	158																
94	S. Atlantic	We	78	Mb	82	Cr	76	Pe	82½	La	33	RJ	38½	Hu	60	Ad	84		

95	S. Atlantic	Mb	77½	La	38	RJ	43												
96	S. Atlantic	We	84	SS	124	La	39½	RJ	41½										
106	SE. of Madagascar	CB	53	We	85¾	Pe	48½	Ba	53½										
107	SE. of Madagascar	CB	53½	We	85¾	Mb	68½	Cr	83	Pe	49	Am	72	Me	54	Ba	53	Co	46	Hu	116
108	SE. of Madagascar	CB	53½	Ba	53	Me	54	Hu	116											Ad	65
112	Mexico	Ho	46½																
116	Near Samoa	Be	69	Vi	74½														
124	Mexico	Ha	36½																
131	Solomon Is.	Si	85																
134	Alaska	Ab	51	Be	29½	St	29½	Li	29¾	Ho	41	Ci	40½	Ot	43¾	Hx	49½	Sa	24½	LR	44
		Fl	41½	SL	41½	Gg	48	SS	45	Ha	47½	Up	58	He	57½						
136	Alaska	Be	29½	St	29¾	Li	30	Ab	56	Up	64½	He	64½								
138	Alaska	Be	28	St	28	He	61	Ab	53	Up	61										
139	Guatemala	Be	36½	St	36	Li	35¾														
154	Alaska	Ot	38½																
155	Mexico	Ot	34	Sa	37	Hx	40	SL	23½										
156	Nevada	Ot	32	Sa	15	Hx	40½	Si	21½	SJ	49½	SL	21¾	Gg	32				
157	Utah	Si	21	Ci	19	LR	17½												
158	Utah	Ci	19	Ot	27½	LR	17½	Fl	17¾	SL	17¾	Gg	27½						

*) Ab = Abisko; Am = Amboina; Ba = Batavia; Be = Berkeley; Ch = Charlottesville; Ci = Chicago; Cr = Christchurch; CB = Colaba-Bombay; Co = Colombo; Fl = Florissant; Gg = Georgetown; Hx = Halifax; Ha = Harvard; He = Helsingfors; Ho = Honolulu; Hu = Huancayo; Iv = Ivigtut; Lz = La Paz; La = La Plata; Li = Lick Observat.; LR = Little Rock; Me = Medan; Mb = Melbourne; Ot = Ottawa; Pe = Perth; RJ = Rio de Janeiro; SL = Saint Louis; SJ = San Juan; Sa = Saskatoon; SS = Scoresby-Sund; Si = Sitka; St = Stanford; Te = Technology; Up = Upsala; Vi = Victoria; We = Wellington; Ad = Adelaide.

From 1 to 108 these are the numbers of Table 1 of the first paper; from 109 to 185 they are assigned to additional shocks given in Table 1 of the present paper. Table 1 and Table 2 also show epicentral distances for all seismograms not used in the first paper.

III. Statistical survey of periods.

There already exists in the literature a considerable body of data on the prevailing periods recorded for various phases. The present investigation has supplied a very large number of additional measurements. Periods for *P*, *PP*, *P'*, *S*, *PKS*, and *SS* have been measured on all seismograms of the Sumatra and Solomon Islands earthquakes. Many other measurements have been made on the Pasadena and Huancayo seismograms of the other shocks used. These data are summarized in Table 3, in which have also been incorporated the results of H. Sommer[2]) on the Alaskan shock of 1927, and of Byerly on the Texas[3]) and Montana[4]) shocks. The tabulation gives for each case those periods which clearly prevail, being found more frequently than other periods for the same phase. Exceptionally well indicated prevailing periods are marked "!"; where a wide band of periods is indicated without evident distinction, this is indicated by giving a range, as 6—8. In Table 4 are given the corresponding results for *P* and *S* as derived from the published bulletins of several stations in recent years. If it is desired to supplement these two tabulations with the results of earlier investigations, reference may be made to Handbuch der Geophysik.

The tabulated data do not include results from the first 2000 km. At these very short distances it is found that there is a regular increase in period with distance, for both *P* and *S*, up to about 2000 km. The corresponding data for the region of Pasadena, with a summary of other published results, will be found in a forthcoming publication by one of us[5]). Beyond 2000 km. the data for the present tabulations show in general no marked effect of distance; where such effects exist, they will be pointed out in the discussion which now follows.

The selection of periods for measurements is unavoidably affected by the constants of the instruments. Those commonly in use tend to accentuate the long periods; while those in service at Pasadena are particularly sensitive to short periods. A clear picture of the true situation can best be had by combining these two groups of data. In general, periods of 2 seconds or less are recorded in teleseisms only in the longitudinal waves (*P*, *PP*, *P'*, etc.).

Table 3. Dominant periods of bodily waves.

Shock	Phase						
	P	*P'* diffr.	*P'*	*PP*	*S*	*SKP*	*SS*
Sumatra Febr. 1931	4! 6—8	1—5	8—9	4 9!	10!(9–11)	8!	28—32
Sumatra Sept. 1931	6—9	2! 6	8	7—9!	8—9	2—8	23—32
Solomon Is. 1931	1—3! 8	2! 5—6	2 5 10	5—8	4 9—11	8!—10	23—30 60
Solomon aftershock	1!						
Texas 1931	2 5—8!			7—9!	8—11		15
Alaska 1927	4—6!			6—8	12—14		14—18
Montana 1925	3!				4!		
Station							
Pasadena	1—3!	1—2	(2—5)	3—4	5—12		
Huancayo	6—8		(5)	6—8	12!		

Table 4. Dominant periods of *P*- and *S*-waves.

	Riverview 1930/34	Cartuja 1932/33	Barcelona 1931/33	Jena 1931/33	Nanking 1932/34	Göttingen 1931/33	La Paz 1932/33
P	2—4	4—6	4—6	2 4 8	3—4	3	2 6
S	5—8	7—9	8	8—9	7	7—10	8 12

In the *P* phase short periods (1—3 sec.) are very frequent under practically all circumstances; periods of 6—8 sec. also are often observed. Longer periods occur; at Pasadena there are a number of observations of periods of 10 sec., at distances less than 30°. In the large Solomon Islands shock, for which the transverse waves usually show quite long periods, the longitudinal waves show periods only up to about 15 seconds; while in the Sumatra shocks, periods of as much as 21 seconds have been measured for *P*.

The diffracted *P'*, which is found at less than the focal distance (142°), is distinguished by marked prevalence of exceptionally short periods (1—2 sec.). Periods of 5—6 seconds are also commonly observed. In the true *P'*, beyond 142°, short periods are much less common; the most usual periods are 8—10 seconds, with a number of cases about 5 seconds and comparatively few about 2 seconds.

The observed periods of *PP* are in general slightly longer than those for *P*. In the Solomon Islands shock periods of 20 seconds and over were found at 115° and beyond. As observed at Pasadena, *P'P'* generally shows periods of about 3—5 sec.

The periods of S are in general slightly less than double the periods of P; this is in agreement with earlier findings. Periods of 30 seconds, or even longer, are occasionally observed. At Pasadena the longer periods are especially noticeable on seismograms from about 50°, about 75°, and about 95°.

The periods of SKP agree more nearly with those of PP than with those of S.

SS and SSS (also, occasionally, PPS and $SKSP$), show very long periods. Those for SS are most commonly from ¼ to ½ minute; in the Solomon Islands shock, at twelve stations distant over 130°, periods of about one minute have been observed. In the Japanese earthquake of March 2, 1933, SS was recorded at Pasadena with a period of well over a minute. Cases of this kind have on a number of occasions led various authors to a mistaken identification of these large, long-period waves with L.

IV. Compressions and dilatations.

The Sumatra shocks of 1931 are recorded with sharp first motion at many stations, so that it is possible to investigate the geographical distribution of initial compressions and dilatations. At all stations where the nature of the first motion can be determined for both shocks, it proves to be the same in both cases. The results are presented in Fig. 1. The distribution of stations for which these data are available is such that any conclusion is rather doubtful; but if it is desired to represent the conditions in a simple way, it is clear that a great circle passing approximately northwest-southeast through the epicenter will separate most of the points where compression is observed from most of those giving a dilatation.

The nature of the first motion at Pasadena for shocks studied in these papers has also been determined. There is clear indication of a geographical distribution of shocks showing initial compression and initial dilatation at Pasadena. This will appear from Table 5, which includes determinations for a number of additional shocks not otherwise used, especially deep focus earthquakes.

The most important result of the tabulation is that the deep-focus shocks clearly show the geographical distribution for recorded initial compressions and dilatations. Where a comparison is possible, the distribution is the same for deep focus shocks as for normal shocks in the same regions. It should be noted that the data are in general better

for deep focus shocks than for normal ones, on account ot the more frequent registration of sharp iP, especially in the vertical component. Only those normal shocks have been used for which the nature of the initial motion was perfectly clear.

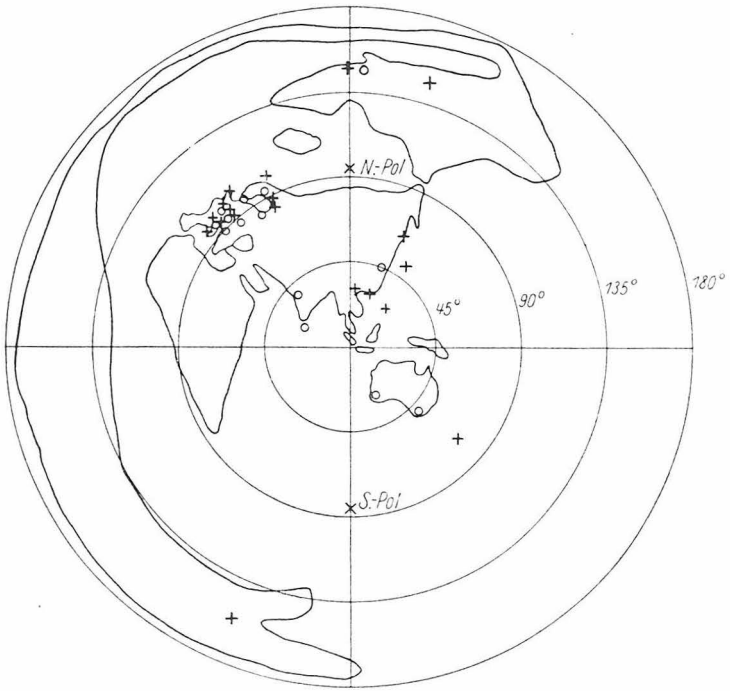

Fig. 1. Compressions (crosses) and dilatations (circles) observed for the Sumatra shocks of 1931.

It will be observed that we record almost exclusively dilatations from the Pacific region of South America. The line in the table reading "Central America, etc.", includes shocks in Northern South America, Central America proper, and Mexico east of the meridian of 105°; these shocks nearly all record with initial compressions. The next group of shocks, from northwestern Mexico (west of 105°), gives dilatations. Shocks within a few degrees of Pasadena show both compressions and dilatations; these are not listed.

From Alaska and the Aleutian Islands we have mostly dilatations. One of the two exceptional compressions is the shock of Feb. 22, 1935,

Table 5.
Compressions and dilatations at Pasadena 1931—1934.

Location	Normal shocks		Deep focus shocks	
	Comp.	Dilat.	Comp.	Dilat.
South America (Pacific coast) . .	1	3	0	15
Central America, etc.	15	1		
Northwestern Mexico	0	3		
Alaska and Aleutian Is.	2	10		
Kamchatka, Kurile Is.			3	1
Manchuria			4	0
Japan	2	2	0	2
Bonin Is.			4	1
Marianne Is.	0	2	1	1
Polynesia (except Samoa)	20	1	10	2
Samoan region	0	2	1	4
Hawaii.	1	0		
Easter Island region	1	1		
Philippines	1	0		
Celebes Sea	1	0	0	1
Baffin Bay	3	0		
Central Asia (Altai)	2	0		

at about 52° N., 176° E.; this is so far west that it may belong to the Asiatic group of shocks giving compressions.

The next few lines of the table show that from the western side of the Pacific (Asia and Polynesia) we record principally compressions. The exceptional dilatations occur most frequently on the oceanic margin of the earthquake belt; the Samoan region is a well marked case of this kind. One of the deep focus shocks showing dilatation, listed with the Polynesian group, occurred at about 11° S., 170° E., which is also within the marginal area.

There appears to be a tendency for large shocks to be exceptional. Thus, the only compression recorded from the Pacific region of South America is the large Iquique shock of Feb. 23, 1933. Also, one of the few dilatations from the Asiatic region is the great Japanese shock of March 2, 1933; its aftershocks, particularly the large one on June 18, gave initial compression. This was true at Uccle as well as at Pasadena. Another case of this kind is the large Alaskan shock of April 27, 1933,

which gave an exceptional compression, at Pasadena; however, it was not exceptional at Uccle, where shocks in this region regularly give compressions. This shock was remarkable for the unusually large number of aftershocks recorded at Pasadena. An opposite case is the shock of May 4, 1934, in the same region, which was not exceptional at Pasadena, showing a large, sharp dilatation, but recorded exceptionally (dilatation) at Uccle. The following stations recorded an initial dilatation for this shock, and an initial compression for the Alaskan shock of July 28, 1394: Upsala, Abisko, Helsingfors, Uccle, Hamburg, Kew, Trieste, Wien, Zi-ka-wei, Chiufeng, Vladivostok, Washington. The first three were determined from original seismograms; the other data are from station bulletins. On May 4 dilatations were also recorded at Honolulu and Chicago (original), and at La Paz, Harvard, Tortosa, Göttingen, Firenze, Zagreb, and Nanking (reports). Cartuja reports a compression.

Two other exceptional cases deserve special notice. One of these is the Central American shock of Dec. 24, 1934, at 14^h; the dilatation recorded at Pasadena is very clear. The other is that of 1933, August 5, 0^h, in the Solomon Islands, which also gives a clear dilatation from a region characterized by compressions. The other exceptional dilatations in the same region are deep focus shocks; one of these originated near the normal shock just mentioned, while the other is that previously referred to as probably belonging to the marginal group of dilatations.

The geographical distribution of recorded initial dilatations and compressions from single earthquakes has been investigated by many authors; the earliest publications were by S. Nakamura, K. Suda, A. Imamura[6]), and P. Byerly[4]). Such investigations throw light on the mechanism of individual shocks. The credit of pointing out that a geographical distribution also exists for earthquakes giving compression and dilatation at a given station belongs to E. Gherzi, who published data establishing this from the records at Zi-ka-wei, in 1923[7]). Similar results were then found at Uccle by O. Somville[8]). The importance of this phenomenon, when supported by the data of stations in different parts of the world, consists in establishing that mechanisms of the same character, and operating in the same direction, must continue to produce earthquakes in the same regions over long periods of time. It is particularly surprising to find, as Table 5 clearly shows, that the deep focus shocks show a geographical distri-

bution for compressions and dilatations, which in general agrees with that for normal shocks.

The Alaskan and Aleutian shocks, although at normal depth, are favorable cases for study, on account of their situation, which results in good seismograms in practically all azimuths. Comparison of the station bulletins for recent years shows that most of these shocks have recorded with initial compressions at practically all stations. In these cases the seven stations in southern California are exceptional in regularly recording initial dilatations. In his first publications[7]) GHERZI reported that shocks from this region regularly give dilatations at Zi-ka-wei. This continues to be evident in the bulletins of that station down to the end of 1929. There were no large shocks in the region during 1930 and 1931. The Zi-ka-wei bulletins give only one case for 1932, which is also a dilatation; but six of the seven shocks in Alaska and the Aleutian Islands during 1933, 1934, and 1935 so far as available, for which the data are given from Zi-ka-wei, have recorded there with initial compressions. The exceptional case is that of May 4, 1934, already mentioned as having given exceptional dilatations everywhere (and the usual dilatation at Pasadena).

Some of the uncertainties in interpreting such data are due to the frequent registration of a small eP followed by a large iP of opposite character. In such cases GHERZI states that he has regularly used the iP; whereas the Pasadena measurements in similar circumstances always refer to eP. A case of this type is the Alaskan shock of October 24, 1927, investigated by H. SOMMER[2]). Initial dilatation was found at most stations in all azimuths; but on the seismograms at Pulkovo and Leningrad, reproduced in the publication, there is clearly an emergent compression preceding the large dilatational iP. Unfortunately, the Pasadena seismograms did not suffice to establish the nature of the first motion.

From the general agreement in all azimuths, it seems that the principal movement in these Alaskan shocks must be vertical. In most cases, where compressions are generally recorded, this movement should be downward at the origin. The recorded dilatation in Southern California indicates that there may also be some horizontal displacement.

Since all these problems, especially that of the connection between normal and deep focus shocks, are of very considerable interest, the recent suggestion of ISHIMOTO that all stations should report the nature

of initial motion is very commendable. However, great caution is required in this matter. The suggestion of GHERZI, at the International Congress of 1925, that *c*, *d* (for compression and dilatation) should be used instead of + and —, has been adopted at Pasadena; it eliminates possible confusion between the motion of the inertia mass and that of the ground, which is a frequent source of error. Such data should be given only when there is little doubt as to the direction of the first wave; otherwise, on small or disturbed seismograms, the wave measured may be a large impulse following, and opposite to, a small emergent beginning. The relatively small number of cases given for Pasadena in Table 5 is due to this precaution.

In a limited number of cases, results of theoretical value may be obtained by comparing the nature (compression or dilatation) of the first recorded motion of *P* with that of reflected longitudinal waves such as *PP* and *PcP* on the same seismogram. Opportunities of this kind are not frequent, since the beginning of the later phase is not always sharp, and is likely to be confused by earlier motion. If the later phase corresponds to a ray which left the hypocenter in a direction not greatly different from that of *P*, the comparison affords a test of the theory of reflection of longitudinal waves at a discontinuity. This condition is fulfilled by *PP* and *PcP*, if the distance is not too small.

The theory has been worked out by KNOTT[13, 14]), ZOEPPRITZ[11]), and JEFFREYS[10]). In the following discussion we shall assume the amplitude of the incident longitudinal wave to be $A_i = 1$; the amplitude of the reflected longitudinal wave is A_r. As has been done in Handbuch der Geophysik, vol. 4*), the convention as to sign differs from that used by ZOEPPRITZ, so that A_r is positive when there is no change of phase on reflection, and negative when the change of phase occurs.

For grazing incidence ($i = 90°$), $A_r = -1$. This general result is independent of the elastic constants and densities of the two media.

For vertical incidence ($i = 0$), for all cases

$$A_r = \frac{\varrho_2 V_2 - \varrho_1 V_1}{\varrho_2 V_2 + \varrho_1 V_1},$$

where ϱ_1, V_1 are the density and velocity of longitudinal waves in the

*) Attention is directed to the following misprints on p. 45 of this volume 4: In (115) the last terms of the third and fourth equations should contain cos 2 i_2 and sin 2 i_2 in place of cos i_2 and sin i_2. In (117) the denominator of f should contain cos i_1, instead of cos 2 i_2.

medium in which the waves are incident, and ϱ_2, V_2 are the corresponding quantities for the other medium. This relation is independent of the velocity of transverse waves in either medium. Thus for vertical incidence there is always a change of phase if $\varrho_2 V_2 < \varrho_1 V_1$, no change of phase if $\varrho_2 V_2 > \varrho_1 V_1$, and no reflected longitudinal wave if $\varrho_2 V_2 = \varrho_1 V_1$.

In the cases of PP, pP, and $P'P'$, where the reflection takes place at the surface of the earth, we have $\varrho_2 = 0$. We then have $A_r = -1$ for both grazing and vertical incidence. The behaviour at intermediate angles depends only on POISSON's ratio σ. For $\sigma = 0.27$, A_r is negative for all angles of incidence[9, 12]); in this case PP should always begin with initial motion opposite to that of P, except in cases of peculiar mechanism at the focus. According to JEFFREYS[10]), for $\sigma = 0.25$, A_r is still negative for most angles of incidence; but it has two zeros at $i = 77.4°$ and $i = 60°$, which occur only very close to the epicenter. Between these limits A_r rises to a maximum of $+0.058$.

Observations for comparison with these results are very scanty; the beginning of PP is almost always confused by other motion, so that conclusions are difficult. See Figs. 4, 5 and 9—11.

In deep focus shocks it is possible to compare the initial motion of the recorded pP with that of P; but it must then be remembered that the corresponding rays usually start in very different directions from the hypocenter, so that one may start as a compression while the other starts as a dilatation. In this case, since pP changes phase at the reflection, pP and P should show parallel initial motion on the seismograms. In the few good instances of deep focus shocks with sharp P and pP as recorded at Pasadena, this appears to be the case.

$P'P'$ starts at an angle of nearly 45° to P, so that the relation between the two waves must be much affected by the mechanism.

In the case of PcP, the ratio of reflected to incident waves can be calculated from the formulas given by ZOEPPRITZ for the case when the velocity of transverse waves is zero in the second medium. The other velocities at the discontinuity can be given the values found in the present paper. It is necessary to make a further assumption as to the ratio of the densities. The two extreme permissible assumptions are $\varrho_2 = \varrho_1$ and $\varrho_2 = 2\,\varrho_1$. (See Handbuch der Geophysik **2**, 462ff.).

The results for $i = 0$ depend only on the ratio $\varrho_2 V_2 / \varrho_1 V_1$, and consequently are independent of assumptions as to the liquid nature of the core. For equal densities, A_r is then about $-1/4$ (change of phase);

in the other extreme A_r is about + 0.1 (no change of phase), for vertical incidence.

Introducing the further assumptions, and examining the case of equal densities, we find that A_r increases with increasing angle i, passes through zero between $i = 30°$ and $i = 40°$ (Δ about 30°), has a maximum of about $+1/4$ near $i = 60°$ (Δ about 55°), is again zero near $i = 80°$, and decreases rapidly to —1 at grazing incidence.

For $\varrho_2 = 2\,\varrho_1$, A_r remains positive up to about $i = 85°$; there is still a maximum about $i = 60°$, where A_r is almost $+ 1/2$. Approaching grazing incidence, beyond 85°, A_r decreases very rapidly to —1.

Since the initial rays of *PcP* and *P* start almost in the same direction (except for very small epicentral distance) *PcP* should show the same initial recorded displacement as *P*, for all except very small and very large distances.

We have a few very good observations of *P* and *PcP* at distances between 30° and 35°, where *PcP* is large. In all these cases *P* and *PcP* show definitely parallel recorded displacements. (See Fig. 10 of the first paper, and Fig. 2 of the present paper.) At distances approaching 90° there are some good seismograms of deep-focus earthquakes, which appear to show the theoretically expected *PcP* with displacement opposite to *P*. In general, the observations agree with theory; the amplitudes appear to correspond more nearly to the expectation for $\varrho_2 = 2\,\varrho_1$ than to that for $\varrho_2 = \varrho_1$. In the case of equal densities, our assumptions lead to a smaller bulk modulus in the core than in the mantle, in the neighborhood of the discontinuity; while the other case gives a slightly higher bulk modulus within the core.

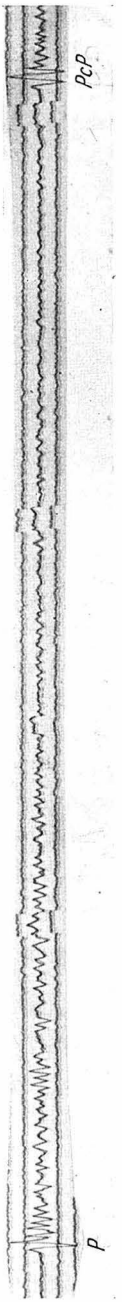

Fig. 2. Shock 139 (Guatemala), recorded at Pasadena (31°). Short-period Benioff vertical.

V. Theoretical considerations on amplitudes, travel times, velocities, and their relation.

The observed amplitudes of bodily seismic waves are interpreted in terms of the theoretical formula

$$(1) \qquad A_e = C\,T \sqrt{\left(\prod_1^n \frac{E_f}{E_e}\right)\left(\prod_1^m \frac{E_r}{E_e}\right) e^{-\int k\,dD} \frac{\tan i}{\sin \Delta} \left|\frac{di}{d\Delta}\right|}$$

where A_e is the true amplitude of the incident wave; C is a constant, which depends on the energy at the source, and which may differ for longitudinal and transverse waves; T is the period; i is the angle of incidence at the observing station; Δ is the angular distance from source to station, both of which are here assumed to lie at the surface of a single sphere. The exponential factor, in which dD is the element of path, represents the absorption; as this is small, and the value of the absorption constant k is not precisely known, this factor is taken as 1 in the following discussion. The other two products which appear under the radical represent the loss of energy occasioned by n refractions and m reflections, respectively.

Any desired component of the displacement at the surface may be obtained by multiplying A_e by a factor which, for longitudinal waves, depends on the angle of incidence, POISSON's ratio in the surface layer, and the direction of the component relative to the plane of propagation. For transverse waves this factor will also involve the polarization. The three components of displacement are usually taken as: u, horizontal in the plane of propagation; v, horizontal perpendicular to the plane of propagation; w, vertical. For longitudinal waves $v = 0$. Values of u/A_e, v/A_e, w/A_e, have been tabulated under special assumptions [12, 10, 9]). Similar tabulations are available for the factors representing loss of energy due to refraction and reflection [11, 13, 14, 15, 16, 17]).

In general the factors u/A_e, v/A_e, w/A_e are smooth functions of i, and consequently of Δ. For longitudinal waves u/A_e is zero for $\Delta = 0$ ($i = 90°$), and increases gradually to a maximum of about 1.66 at a distance of a few degrees, for which i is about 60°; it then decreases to about 1.4 for $i = 43°$, 1.0 at $i = 27°$, etc., reaching zero at the antipodes of the epicenter. w/A_e also is zero for $\Delta = 0$, and increases gradually to a value of 2 at the antipodal point. In the case of transverse SV-waves at short distances the conditions are complicated; for distances over 40° u/A_e is about 2 [9, 10]). For SH, u and w are zero, while $v/A_e = 2$.

The refraction factors in the expression for A_e depend very much on the elastic constants and densities at the refracting discontinuities. In general they change gradually with Δ, but abrupt changes occur when any of the refractions take place near a critical angle. There is a similar behaviour of the reflection factors for reflections in the interior of the earth; but the factor E_r/E_e changes gradually when the reflection is at the surface of the earth, beginning with the value 1 at $\Delta = 0$ and decreasing to a very small minimum for i between 65° and 75° (the corresponding Δ depends on the local structure of the upper layers), after which it increases slowly to 0.5 for $i = 27°$ and 1.0 at the antipodal point — all these numerical values applying to longitudinal waves only. For further details see section IV.

The factor $\tan i/\sin \Delta$ occasions no irregularities; but the formula (1) for the amplitudes contains $di/d\Delta$. In many cases it is this factor which determines the behavior of the amplitude as a function of distance, since it often changes much faster than the other quantities involved. Consequently, it is advantageous to investigate the relation of this derivative, and of the corresponding second derivative, to the observed travel times.

In the following discussion we shall use polar coordinates r, θ, Φ with origin at the center of the earth. At the surface we have the relation $\Delta = r_0\theta$, where r_0 is the radius of the earth. The use of θ instead of Δ simplifies the equations, and makes them applicable at all depths. The earthquake focus, however, is taken as at zero depth. The time t is the actual elapsed time from the occurrence of the shock to the arrival of the disturbance at the point (r, θ). The surface $t =$ constant therefore is the wave front. The rays are of course orthogonal to these wave fronts; and we may specify any given ray (apart from azimuth) by any quantity which is constant along the ray. Such a quantity is r_s, the value of r at the deepest point of the ray. (r_s, t) then constitute an orthogonal system of coordinates which describe the points of the space as adequately as (r, θ). In addition, we define the angle of incidence i, which is the angle between the ray and the radius vector at the point considered. The velocity v is taken as a function of r only; v_s denotes the value of v for $r = r_s$, and v_0 the value at the surface $(r = r_0)$.

We shall make much use of partial derivatives with respect to the several variables, and to avoid confusion we shall use the notation which explicitly indicates the quantities which are held constant as

well as those which are varied. As abbreviations we define $t' = (dt/d\theta)_r$ and $t'' = (d^2t/d\theta^2)_r$, etc. We also write $\bar{v} = r/t'$; at the surface, putting $r = r_0$, this becomes the observed apparent surface velocity.

The fundamental equation from which the following results are derived is

$$t' = \frac{r}{v}\sin i = \frac{r_s}{v_s}. \tag{2}$$

From this, differentiation leads to

$$\left(\frac{di}{d\theta}\right)_r = \frac{t''}{t'}\tan i\,, \tag{3}$$

$$\left(\frac{d^2i}{d\theta^2}\right)_r = \left(\frac{t''}{t'}\right)^2 \tan^3 i + \frac{t'''}{t'}\tan i\,, \tag{4}$$

$$\left(\frac{d^2\theta}{di^2}\right)_r = -\frac{t'}{t''} + \frac{(t')^2\,t'''}{(t'')^3}\cot^2 i\,. \tag{5}$$

Since $\sin i > 0$ (except for the ray passing through the center of the earth) we have from (2) that

$$0 < t' \leqq \frac{r}{v}\,, \tag{6}$$

so that if θ is neither 0 nor 180°, t' cannot be zero, and is always finite and positive. For $r = r_0$, t as a function of Δ $(= r_0\theta)$ is the normal travel time curve; so it follows that:

The travel time curve can have neither maxima nor minima (between 0° and 180°), nor vertical tangent; t always increases with increasing Δ.

By definition

$$\bar{v} = \frac{r}{t'}\,, \quad \text{whence} \quad \left(\frac{d\bar{v}}{d\theta}\right)_r = -\frac{r\,t''}{(t')^2}\,. \tag{7, 8}$$

From (6) it follows that $\bar{v}$ (which for $r = r_0$ is the apparent surface velocity) can be neither zero nor infinite between $\theta = 0$ and $\theta = 180°$, and is always positive:

$$v_0 \leqq \bar{v} < \infty \quad (\text{for } r = r_0)\,.$$

For any given r there cannot be two values of θ corresponding to any given value of i; for $r \sin i/v$ is constant along each ray, so that two values of θ would then correspond to the same i at the source. That is, the rays would branch at some point, which contradicts Snell's law if v is a function of r only. Hence, between $\theta = 0$ and $\theta = 180°$ there can be no maxima or minima of i at constant r:

$$\left(\frac{di}{d\theta}\right)_r \neq 0\,.$$

Since $\left(\frac{di}{d\theta}\right)_r$ is negative at $\theta = 0$, it is negative for all values of θ if i is a continuous function of θ and $\left(\frac{di}{d\theta}\right)_r$ is nowhere infinite.

Since $\left(\frac{di}{d\theta}\right)_r \neq 0$ it follows from (4) that $t'' \neq 0$, since the possibility of $t' = 0$ has already been excluded. Hence:

The travel time curve can have no point of inflection.

From (8) it then appears that $\left(\frac{d\bar{v}}{d\theta}\right)_r \neq 0$, whence:

The apparent velocity can have no maximum or minimum as a function of Δ.

If $\bar{v}$ is continuous from $\theta = 0$ to $\theta = \theta_1$ and its derivative does not become infinite in that interval — $\bar{v}$ always increases with θ — the apparent velocity increases with distance between 0 and θ_1.

It should not be overlooked that the travel time curve may consist of several branches; it may be broken into discrete segments, or even single points. This has recently been discussed by SLICHTER[18]).

Although $\left(\frac{di}{d\theta}\right)_r$ cannot become zero, as we have seen, it may become very small; this requires that t'' be small while t' remains finite — that is, the travel-time curve has a very large radius of curvature (approaches a straight line). From (1) it follows that in this case the amplitudes are very small; a nearly straight travel-time curve is inconsistent with large amplitudes.

It may also happen that t'' becomes very large; then the radius of curvature of the travel-time curve is very small, so that it has a cusp or a sharp change in direction. $\left(\frac{di}{d\theta}\right)_r$ then becomes very large; from (1) it then follows that in general (subject to exceptional behaviour of the other factors involved) the amplitudes will be very large. By definition, an infinite value of $\left(\frac{di}{d\theta}\right)_r$ corresponds to a focal point; for in this case rays leaving the source with successive values of i arrive at the same point. The well-known focus of P' corresponds to the case of a cusp in the travel-time curve. A case of the sharp change in direction of a single-valued travel time is given by SLICHTER[18]) in section 2.2 of his paper. In both cases the apparent surface velocity curve has a vertical tangent.

Another special case occurs when t''' becomes infinite but t'' re-

mains finite. From (1) and (4) it will be seen that $\left(\frac{d^2 i}{d\theta^2}\right)_r$ and $\left(\frac{dA}{d\theta}\right)_r$ become infinite; the amplitudes change discontinuously with distance. In terms of the behaviour of the travel-time curve this corresponds to a rapid change in the radius of curvature; the apparent velocity curve has a sharp change in direction.

It is of much interest to inquire what behaviour of the velocity v as a function of depth corresponds to the various special cases which have been described for the amplitudes, the travel-time curve, and the apparent surface velocity curve. For this purpose we have to express v_s as a function of r_s, and discuss the derivatives $\frac{dv_s}{dr_s}$ and $\frac{d^2 v_s}{dr_s^2}$. Since v_s depends on r_s only, these are total derivatives; but we express them in terms of partial derivatives. In particular

$$\frac{dv_s}{dr_s} = \frac{\left(\frac{dv_s}{d\theta}\right)}{\left(\frac{dr_s}{d\theta}\right)}. \tag{9}$$

Applying this to (2), we find

$$\frac{dv_s}{dr_s} = \frac{1}{t'} - \frac{r_s t''}{(t')^2 \left(\frac{dr_s}{d\theta}\right)_r} = \frac{1}{t'} - \frac{t''}{(t')^2 \left(\frac{d \log r_s}{d\theta}\right)_r}. \tag{10}$$

The functional relation between r_s and θ at constant r is given by the well-known integral equation

$$\log \frac{r_0}{r_s} = \frac{1}{\pi} \int_0^{\Theta} q\ (\theta, x)\, dx\,, \tag{11}$$

where

$$\cosh q = \frac{t'\,(x, r)}{t'\,(\theta, r)}. \tag{12}$$

(A discussion and references can be found in Handbuch der Geophysik, vol. 4.)

The usual notation is here clarified by using x instead of θ for the variable of integration and retaining θ only for the limit of integration. The fact that q is really a function of these two variables is important in carrying out the differentiations which follow. To make the calculations apply equally at all depths we have retained θ instead of introducing Δ; this has the effect that r_0 drops out of the later equations.

The integral equation (11) is the final result of a complicated mathematical procedure; so that before using it to draw physical conclusions it is necessary to establish the precise conditions for its vali-

dity. This has recently been discussed very carefully by H. WITTE[19]), and independently by L. SLICHTER[18]), who has shown how to extend the method to cover cases excluded by WITTE.

As pointed out by WITTE, the necessary conditions fall into two groups: Those which must be satisfied in order that the solution may be reduced to that of an Abelian integral equation, and those which must be satisfied in order that the solution may be obtained in the form (11). Making use of the additional results of SLICHTER, it appears that both sets of conditions are completely satisfied in all cases where the travel time is a continuous function of the central angle. Discontinuity by becoming infinite is of course physically impossible; in case of a finite discontinuity the method applies from $\theta = 0$ up to the discontinuity. While WITTE excludes multiple points and cusps, which are not cases of discontinuity in the travel time curve, SLICHTER's procedure covers these cases.

From (10) and (11) we find

$$\frac{d v_s}{d r_s} = \frac{1}{t'} + \frac{t''}{(t')^2} \frac{\pi}{\frac{\partial}{\partial \theta} \int_0^\theta q(\theta, x)\, d x}. \tag{13}$$

Since $q(\theta, \theta) = 0$, we can differentiate the integral by merely differentiating the integrand, so that we have to evaluate $\left(\frac{d q}{d \theta}\right)_x$. We find

$$\left(\frac{d q}{d \theta}\right)_x = - \frac{t''(\theta, r)}{t'(\theta, r)} \frac{t'(x, r)}{\sqrt{[t'(x, r)]^2 - [t'(\theta, r)]^2}},$$

whence

$$\frac{d v_s}{d r_s} = \frac{1}{t'(\theta, r)} \left[1 - \frac{\pi}{I}\right], \tag{14}$$

where

$$I = \int_0^\theta \frac{d x}{\sqrt{1 - \left[\frac{t'(\theta, r)}{t'(x, r)}\right]^2}} = \int_0^\theta \coth q(\theta, x)\, d x. \tag{15}$$

Note that I is a function of θ only.

Similarly we can derive

$$\frac{d^2 v_s}{d r_s^2} = - \frac{\pi}{I r_s} \frac{d v_s}{d r_s} + \frac{\pi^2}{r_s t''(\theta, r)} \frac{\frac{d I}{d \theta}}{I^3}. \tag{16}$$

We first consider equation (14). It is evident that I is always positive; for we have to take the positive branch of the radical, as this

corresponds to taking q positive, which is necessary for the validity of the integral equation (11). Hence

$$\frac{dv_s}{dr_s} \leqq \frac{1}{t'(\theta, r)} \qquad \frac{dv_s}{dr_s} \leqq \frac{\bar{v}}{r}. \tag{17}$$

This leads to several important physical conclusions. It should be noted that a negative value of dv/dr refers to an increase of velocity with depth; so that the inequality (17) sets a limit to the rate of decrease of velocity with depth. That is, if the travel time curve is continuous, the velocity cannot decrease, at a depth specified by r_s, at a faster rate than $\bar{v}/r$. Near the surface $\bar{v}/r$ is numerically small, so that if the observed travel time curve is considered to be continuous there can be only a very slow decrease of velocity with depth in the mantle. Thus for $\bar{v} = 10$ km./sec. v_s cannot decrease with depth at a faster rate than 0.1 km./sec. in about 60 km. without producing an interruption in the travel time curve (a so-called shadow zone). Thus a discontinuous travel time curve may arise from a continuous distribution of velocity with depth, if the velocity at any depth decreases with depth at a faster rate than the limit given by (17). These considerations of course set no limit to the rate of increase with depth. The problem has been investigated in detail by H. Jung[20]).

In the limiting case $dv_s/dr_s = 0$, which occurs when I becomes infinite, the lowest segment of the ray is an arc of a circle $r =$ constant.

We have next to consider the conditions under which I remains finite or becomes infinite.

The integrand is regular except at $x = 0$, where it has a singularity; it is only necessary to investigate the integral in the neighborhood of this singularity. When this is done, it is found that when $t' \neq 0$ I becomes infinite whenever $t'' = 0$. The first condition is always satisfied, as we have shown previously. Now if $t''' \neq 0$, $t'' = 0$ corresponds to a point of inflection in the travel time curve, which has also been excluded; so that the only physical case of this type occurs when both $t'' = 0$ and $t''' = 0$. The curve then has a tangent of high order. The conditions are of course also satisfied by a rectilinear travel-time curve. In these cases, as we have seen, the amplitudes are zero, and the change in velocity with depth is given by $dv_s/dr_s = \bar{v}/r$.

If neither t' nor t'' is zero, and none of the derivatives are infinite, I remains finite. That is, if $t(\theta)$ and all its derivatives are continuous, and t' and t'' do not vanish, from $\theta = 0$ to $\theta = \theta_1$,

then the velocity v is a continuous function of depth down to the level r_s reached by the ray corresponding to θ_1.

If any of the derivatives become infinite, the value of I depends on the manner in which infinity is approached as x approaches θ. An infinity in t' is excluded physically. If t'' is infinite the travel time curve has one of several peculiar types of discontinuity, which have partly been discussed by SLICHTER[18]); the applicability of the formulas (14) and (16) must be discussed separately for each such case, as $\left(\frac{dr_s}{d\theta}\right)_r$ then becomes infinite. Infinities of the higher derivatives are of little practical importance, as they could not be established from observations of travel times.

In discussing the formula (16) for the second derivative d_2v_s/dr_s^2, it is found that in general this remains finite when the first derivative dv_s/dr_s is finite. The only exception of interest occurs when t''' becomes infinite. That is, a discontinuity of the second order in the velocity as a function of depth occurs when the travel-time curve has a discontinuity of the third order (the curvature changes discontinuously), or the apparent velocity curve has a discontinuous change in slope. As pointed out before, in this case the amplitudes also change discontinuously.

Summarizing, we find that since t' is neither zero nor infinite, the important special cases depend on the behavior of t'' and t'''; they may be stated as follows:

$$(18)\quad t''\to 0 \qquad \left(\frac{d\bar{v}}{d\theta}\right)_r\to 0 \qquad \frac{di}{d\theta}\to 0 \qquad A\to 0 \qquad \frac{dv_s}{dr_s}\to\frac{\bar{v}}{r}.$$

$$(19)\quad t''\to -\infty \qquad \left(\frac{d\bar{v}}{d\theta}\right)_r\to\infty \qquad \frac{di}{d\theta}\to -\infty \qquad A\to\infty \qquad \text{singular cases.}$$

$$(20)\quad \begin{cases} t'''\to\pm\infty \\ t''\neq 0 \end{cases} \quad \begin{cases} \left(\frac{d^2\bar{v}}{d\theta^2}\right)_r\to\mp\infty \\ \left(\frac{d\bar{v}}{d\theta}\right)_r\neq 0 \end{cases} \quad \begin{cases} \frac{d^2i}{d\theta^2}\to\pm\infty \\ \frac{di}{d\theta}\neq 0 \end{cases} \quad \begin{cases} \frac{dA}{d\theta}\to\pm\infty \\ A\neq 0 \end{cases} \quad \begin{cases} \frac{d^2v_s}{dr_s^2}\to\pm\infty \\ \frac{dv_s}{dr_s}\neq\frac{\bar{v}}{r} \end{cases}.$$

The case $t'''=0$ is of no particular importance.

VI. Theory of the amplitude ratio PP/P. Effect of crustal structure.

The formula (1) gives A_e as a function of Δ only, as the other quantities included are either functions of i, and therefore of Δ, or are taken to be constant. It is clear that this neglects the ellipticity of the earth; further, because of the difference in structure of the upper layers

in different regions, practically all of the quantities involved in the formula will depend on the particular structures near the epicenter and the station, and in case of reflected waves, at intermediate points. These circumstances may cause the distance Δ, for which the ray considered penetrates to a given depth, to vary by several degrees for a direct ray; the extent of the variation possible is multiplied at each reflection. The change in Δ is a sum of terms of the form d (tan i_1 — tan i_2) where d is the thickness of a crustal layer and i_1, i_2 are the mean angles of incidence for this layer. Thus this effect will be larger for larger values of i, which occur at short distances. The value of i is much affected by the crustal structure, as sin i is proportional to the velocity in each layer. All the other quantities involved in A_e are functions of i. As previously mentioned, the values of some of these quantities are very sensitive to small changes in i when that angle is near certain critical values. At distances corresponding to these critical values, comparatively small changes in crustal structure will produce changes in i which will express themselves in large changes in A_e.

It chances that most observing stations are located in regions of about the same crustal structure (continental type); so that, except for certain Pacific stations, such effects due to difference in location of the station will be relatively small. This also applies to the factors u/A_e, which are required for comparison with observation. Except at very short distances, u/A_e increases and w/A_e decreases with increasing velocity in the principal surface layer, for longitudinal waves.

The difference between continental and Pacific structure in the epicentral region produces an appreciable effect only at rather short distances. As already pointed out, the change in angle of incidence has the effect of a change in Δ. If the earthquake source is within the continental crustal layers, there is a loss of energy due to refraction in passing out of these layers, which of course does not exist when the shock occurs in the Pacific region. For longitudinal waves this loss of energy may be very large at short distances, but it rapidly becomes inappreciable with increasing distances; at $\Delta = 20°$ it is about one quarter, which reduces A_e by somewhat more than 10%.

Difference between continental and Pacific structure at a point where the wave is reflected at or near the surface of the earth may affect the amplitude considerably more. The effect due to change in angle of incidence is doubled; that due to loss of energy on refraction is squared; and there enters a new effect due to loss of energy on re-

flection. Further, in the case of a continental reflection there are two principal levels of reflection — one at the actual surface, the other at the base of the continental layer. JEFFREYS[10]) has calculated that at short distances the PP wave reflected from the base of the continental layer is stronger than that from the surface. In comparing theoretical amplitudes for the PP wave reflected at a continental point at given distance with the corresponding reflection at a Pacific point, care must be taken to use the larger of the two continental reflections. Calculation using the best data available shows that PP from a Pacific reflection should always be smaller than the larger of the two continental reflections at the same distance. The ratio of amplitudes should decrease from about $^1/_2$ at $\Delta = 30°$ to about $^1/_4$ at 45°, then increasing to $^1/_2$ at about 50°, $^3/_4$ at about 60°, approaching 1 for large distances.

Analogous considerations apply when the station or a point of reflection is located in a region where there are deep layers of sediments with smaller wave velocities than those in granitic rock.

The most direct method of applying the formula (1) would consist in comparing the amplitudes of a single wave (say P) of the same shock, as recorded at various distances. This procedure is not satisfactory in practice, for a number of reasons. Thus, there are wide limits of error in calculating the true motion of the ground from seismographic amplitudes, even when the constants of the instruments are determined with all ordinary care and precision. The recorded amplitudes are also considerably affected by the character of the ground on which the station is situated. Lastly, the use of formula (1) implies that energy is radiated equally in all directions from the earthquake focus, — an assumption which is always doubtful, and in some cases is demonstrably erroneous. This has been emphasized by several investigators, notably by KAWASUMI and YOSIYAMA[21]).

For these reasons K. ZOEPPRITZ[12]) suggested the use of the ratios of the amplitudes of different phases as recorded on the same seismogram. This eliminated, to a considerable extent, the uncertainties due to instruments and ground, provided that the phases being compared do not differ greatly in period. The most favorable data for this purpose are provided by the amplitude ratio PP/P. Since these two waves leave the source in the same azimuth, and with angles of incidence which differ only slightly, the effect of irregular radiation of energy is also reduced in this case. Extreme effects of this kind may occur if either ray coincides initially with a direction in which the radiation

of energy is a minimum; but in this case both P and PP are small, and such data are not used in practice.

The ratio of the vertical to the horizontal component for longitudinal waves arriving at the surface depends only on the angle of incidence and POISSON's ratio for the surface layer. (In the case of transverse waves the polarization is also involved.) Thus, for P or PP we have

(21) $$u/w = \tan 2\,a, \text{ where}$$

$$\sin a = \sqrt{\frac{1/2 - \sigma}{1 - \sigma}} \sin i.$$

σ being POISSON's ratio. Thus $\sin a / \sin i$ is the ratio of the velocity of the transverse wave to that of the corresponding longitudinal wave. As $\sin i$ is always larger for PP than for P, u/w is also larger for PP:

$$\frac{u_{PP}}{w_{PP}} > \frac{u_P}{w_P}, \quad \text{whence} \quad \frac{u_{PP}}{u_P} > \frac{w_{PP}}{w_P}.$$

That is, the ratio PP/P is larger in the horizontal than in the vertical component. A factor F for reducing the ratio observed in the vertical component to that in the horizontal component can be calculated from formula (21). (See Fig. 6.)

VII. Observations of PP/P.

A. Continental reflections. Fig. 6 gives observations for PP/P where the point of reflection is continental. Such data were first published by ZOEPPRITZ, GEIGER, and GUTENBERG[12]) giving results at Göttingen for the period 1904—1911. These observations are plotted as circles and squares. Additional data concerning waves with continental paths have been used by GUTENBERG[42]); these are plotted as diagonal crosses, and are listed in detail in Table 6. One shock previously used, the Ferghana earthquake of Nov. 15, 1921, has now been omitted; it proves to have been a case of deep focus, and consequently yielded anomalous results. The erect crosses in Fig. 6 represent observations for the Sumatra shocks of 1931; the numerical data are given in Table 7. The remaining points are from seismograms of recent years at Pasadena, its auxiliary stations, and Huancayo, together with selected seismograms kindly lent us by the directors of other stations, as listed in Tables 1 and 2. The numerical data are given in Tables 8 and 9.

At distances up to 3000 km. (27°) PP is usually very small (see Figs. 3 and 5a). Occasional large waves following P (see Fig. 3c) are

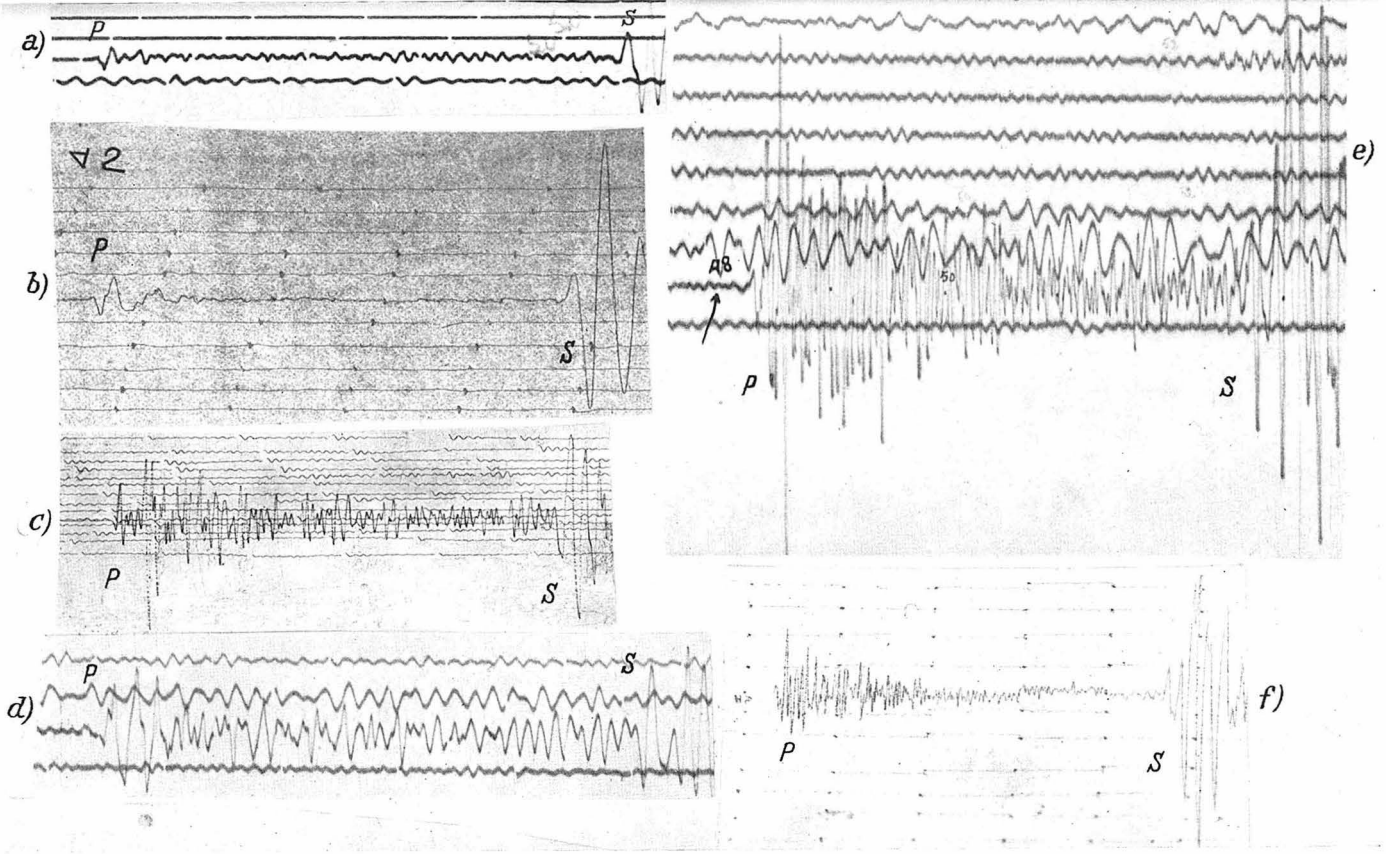

Fig. 3. Seismograms with continental reflections, distance under 29°, showing no clear *PP*. (a) No. 1, Texas-Ottawa NS, 21°; (b) No. 1, Texas-Charlottesville EW, 22½°; (c) No. 134, Alaska-Saskatoon EW, 24½°; (d) No. 134, Alaska-Berkeley EW, 28°; (e) and (f) No. 24, Colombia-La Paz, 25¼°; (e) GALITZIN EW; (f) WIECHERT NS.

frequently too early for PP, and are probably late members of the P group (or possibly pP, etc.). Between 3000 and 4500 km. (27° and 41°)

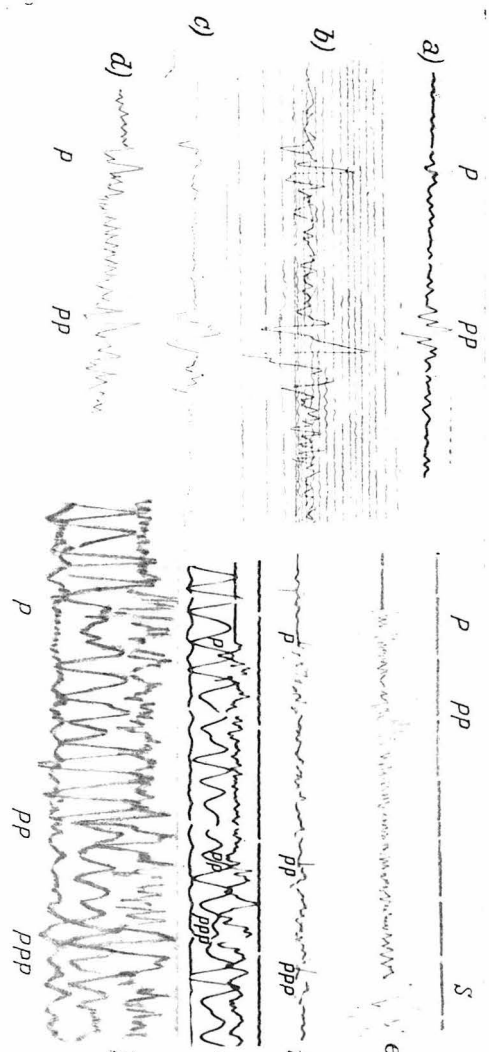

Fig. 4. Seismograms with reflections in North America, showing PP and PPP. (a) No. 3, Mexico-Ottawa NS, 35½°; (b) No. 155, Mexico-Saskatoon NS, 37°; (c) No. 155, Mexico-Halifax EW, 40°; (d) No. 124, Mexico-Harvard Z, 37°; (e) No. 134, Alaska-Chicago EW, 40½°; (f) No. 3, Mexico-Sitka EW, 44°; (g) No. 11, Alaska-Ottawa NS, 44°; (h) No. 11, Alaska-Technology EW, 48½°.

PP is usually larger than P (Figs. 4 and 5b to 5e). At 4500 km. P becomes very small, so that the ratio PP/P suddenly becomes very large; this ratio then decreases to about 7500 km. (67°). Here P again de-

creases somewhat, but thereafter increases with increasing distance, so that the ratio PP/P reaches a minimum about 8400 km. (75°). At larger distances the points scatter very much; apparently in the immediately following range P decreases considerably, but PP also decreases, corresponding to the decrease in P at 4500 km. At about 11500 km. (104°) P decreases very considerably (beginning of the shadow zone).

The plotted observations plainly show more or less scatter at all distances. Apart from errors in measurement and in determination of distance, there are several physical causes which may contribute to this. PP and P leave the hypocentre in slightly different directions, so that the observed ratio may be affected by the mechanism of the shock. In addition, there are possible effects due to the ellipticity of the earth, and to slight differences in depth of focus or in crustal structure near the focus, the station, or the point of reflection. Finally, PP usually has longer prevailing periods than P; this may lead to an appreciable difference in magnification, so that PP/P appears too small on short-period instruments.

Table 6.

Observed values PP/P, horizontal, continental reflections

Japan, September 1923				Japan, September 1923			
Station	Δ	PP/P 1.	2.	Station	Δ	PP/P 1.	2.
Upsala	8170	0.3		Hohenheim	9390	1.0	
Potsdam	8960	1.5		Ravensburg	9500	0.8	
Hamburg	8990	2.5	2½	Zürich	9610	1.1	
Wien	9140	1.1	1.6	Barcelona	10420	9.8	
Jena	9140	0.9		Cartuja	11090	4	
De Bilt	9320	2	1½	San Fernando	11280	> 10	
München	9380	2	1½				

Kamchatka, Oct. 18, 1920			Kamchatka, Oct. 18, 1920		
Station	Δ	PP/P	Station	Δ	PP/P
Potsdam	8170	0.15	Jugenheim	8600	0.34
Göttingen	8380	0.25	Heidelberg	8640	0.33
Jena	8410	0.25	Durlach	8680	0.33
Taunus	8560	0.2	Karlsruhe	8690	0.5
Wien	8560	0.4	München	8700	0.7

Table 6 (continued).

Kansu, December 16, 1920 Station	Δ	PP/P	Kansu, December 16, 1920 Station	Δ	PP/P
Upsala	6600	0.5	Taunus	7550	0.9
Königsberg	6650	0.7	Jugenheim	7600	1.2
Wien	7200	0.6	Heidelberg	7650	1.0
Hamburg	7300	1.0	Hohenheim	7650	1.0
Jena	7400	0.7	Durlach	7700	0.5
München	7500	1.0	Zürich	7750	1.2

Table 7.

Observed values PP/P, horizontal, continental reflections, from the Sumatra shocks, 1931, February 10 and September 25.

Station	Δ	PP/P Feb.	PP/P Sept.	Station	Δ	PP/P Feb.	PP/P Sept.
Melbourne	50.5°	1	1	Jena	94.5		2½
Sverdlovsk	70.4	0.8		Hamburg	95.5	3	4
Pulkovo	85.5		1¾	Stuttgart	96.0	2	2
Beograd	87.9		2	Heidelberg	96.3		3
Helsingfors	88.2	1	1½	Taunus	96.5		3
Budapest	89.3		1¼	Strasbourg	96.9		2
Königsberg	89.5		1½	Neuchâtel	97.5		1¾
Wien	91.2	2		De Bilt	98.5	1½	1½
Zagreb	91.2	1	1½	Uccle	99.0		3
Abisko	92.3	1	2	Paris	100.4		2
Potsdam	93.6	2	1	Kew	101.9		4
Lund	93.7		2	Edinburgh	103.0		1¾
Leipzig	94.0		2	Scoresby Sund	105.7		7
København	94.2	1.1	1.1	Toledo	105.9		15
München	94.3		1¼	Victoria	121.8		8
Firenze	94.3	4	3	Berkeley	127.8		30
Innsbruck	94.4		5				

Table 8. Observed values of PP/P, horizontal (vertical observations are reduced by means of equation 21) with continental reflections from shocks listed in table 4 of the first paper and in table 1 of the present paper and recorded at Pasadena.

No.	Epicenter	Δ	PP/P	No.	Epicenter	Δ	PP/P
14	Centr. America	4100	1.1	22	Baffin Bay	5100	2
17	Cuba	4450	2	120	Kansu	11000	4
23	Newfoundland	5300	0.6	125	Baffin Bay	5100	1±
46	E. Atlantic	8670	1.1	139	Guatemala	3400	≦0.3
73	Kansu	11100	4	144	Baffin Bay	5100	1.0
80	Szechwan	11450	5	10	Centr. America	3770	2½
86	Burma	12300	12	153	Honduras	3750	1½
89	India	12800	40	180	Nicaragua	3800	1¾

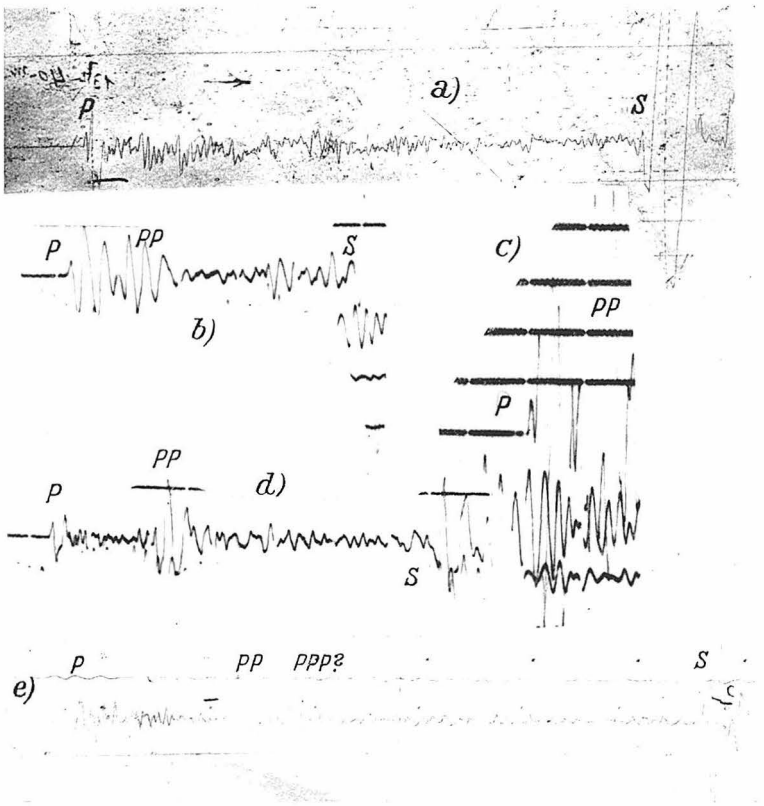

Fig. 5. Seismograms with reflections in South America, showing no PP at 24 ¼°, and large PP at distances over 27°. (a) No. 37, Peru-La Plata EW, 24 ¼°; (b) No. 49, Chile-Rio de Janeiro EW, 27 ½°; (c) No. 50, Chile-Rio de Janeiro EW, 29°; (d) No. 25, Ecuador-Rio de Janeiro EW, 41°; (e) No. 25, Ecuador-La Plata NS, 38°.

B. Pacific reflections. We have seen that PP from Pacific reflections should theoretically be weaker than PP from continental reflections at the same distances especially below 6000 km. This is confirmed by observation, as appears from comparison of Fig. 6, for continental reflections, with Fig. 7, for Pacific reflections. The data of Fig. 7 are all new; they are given in Tables 10 and 11. Typical seismograms are reproduced in Fig. 8. The general behaviour of PP/P as a function of distance is about the same in Fig. 7 as in Fig. 6; the curves in Fig. 7 have been drawn to correspond with those of Fig. 6, and it will be seen that they are not in conflict with the observations.

Apparent exceptions are the seismograms at Huancayo of certain shocks in the eastern Pacific, with reflections south of the Galapagos Islands. (All reflections from the ocean floor north and northeast of the Galapagos Islands are clearly of Pacific type.)

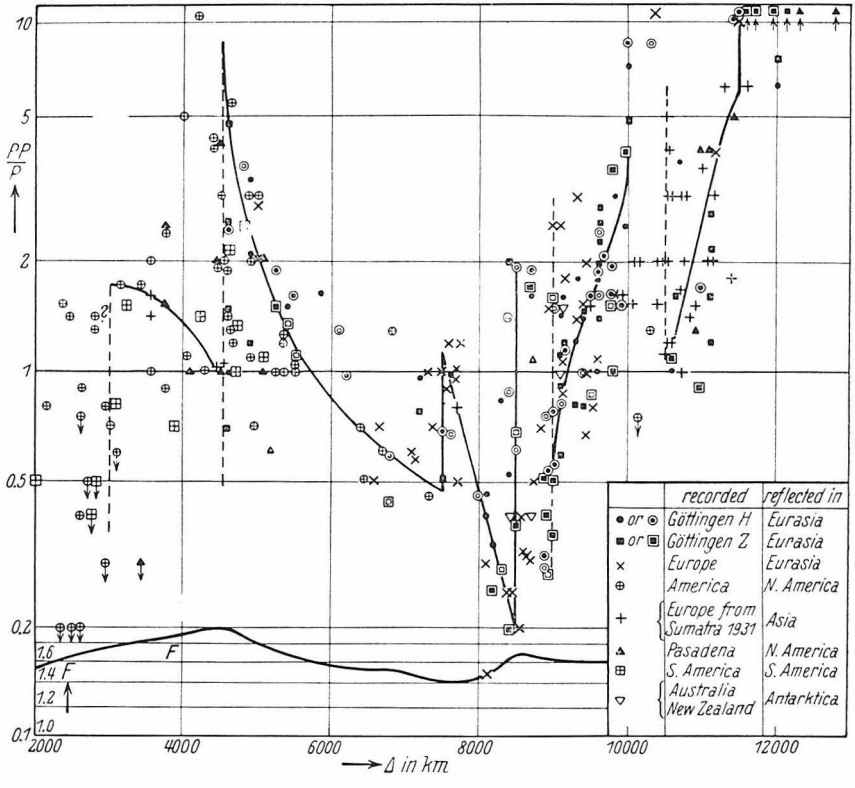

Fig. 6. PP/P for continental reflection.

Double circles and double squares refer to Göttingen. $F = \frac{u_{PP}}{u_P} \frac{w_{PP}}{w_P}$.

The two clearest cases are as follows:

No. 182 1934 April 9, 15^h. 37° S. 98° W. 3600 km. $PP/P = 2\frac{1}{4}$.

No. 183 1934 Feb. 20, 3^h. 6° S. 106° W. 3500 km. $PP/P = 3\frac{1}{2}$ (Fig. 9)

A less positive case is:

No. 15 1932 Nov. 2, 11^h $24\frac{1}{2}$° S. 113° W. 4200 km. $PP/P = 1.7$.

In all three cases PP/P is large, even for continental reflection. However, in the last case the observation might belong to the maximum of PP/P at 4500 km. The corresponding point is plotted in Fig. 7;

but the two preceding cases have not been plotted anywhere. The points of reflection in the three cases are near 25° S. 85° W., 9° S. 91° W., and 20° S. 93° W., respectively. These results appear to indicate that a continental structure exists under the ocean floor in the region in question. This is not unreasonable, since there are numerous

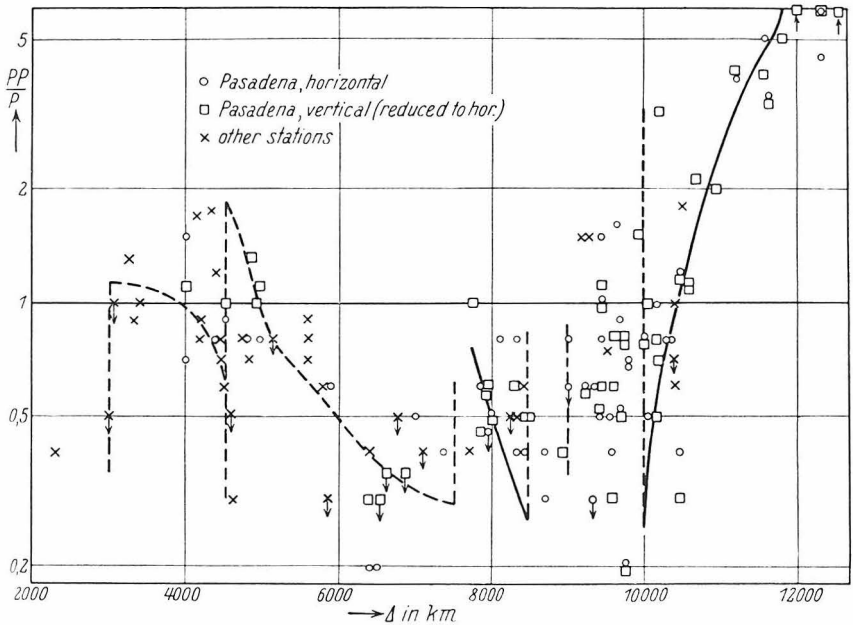

Fig. 7. PP/P for Pacific reflection.

Table 9. Observed values PP/P, horizontal, with continental reflections from shocks listed in table 4 of the first paper and in table 1 of this paper.

a) Reflections in North America.

No.	Epicenter-station	Δ	PP/P	No.	Epicenter-station	Δ	PP/P
154	Alaska-Ottawa . .	4300	1.0	156	Nevada-Halifax .	4480	2
155	Mexico-Ottawa . .	3770	0.9	3	Mexico-Ottawa . .	3945	5
155	Mexico-Saskatoon	4090	1.9	3	Mexico-Saskatoon	3735	2½
155	Mexico-Halifax .	4420	4	1	Texas-Charlottesv.	2480	0
139	Guatemala-Berkel.	4050	1.1	11	Alaska-Charlottes-		
156	Nevada-Ottawa .	2560	1.0		ville	5350	1.0

Table 9 a) Reflections in North America (continued).

No.	Epicenter-station	Δ	PP/P	No.	Epicenter-station	Δ	PP/P
3	Mexico-Sitka . .	4920	0.7	159	Mexico-St. Louis .	2600	0.1
157	Utah-Sitka . . .	2320	0	3	Mexico-St. Louis .	2600	0.9
156	Nevada-San Juan	5510	1.1	11	Alaska-St. Louis .	4650	1.2
3	Mexico-San Juan.	4000	$\frac{1}{2}$	6	Mexico-St. Louis .	2800	1.3 ?
6	Mexico-Chicago USCGS	3150	$1\frac{3}{4}$	134	Alaska-St. Louis .	4600	1.4
134	Alaska-Chicago USCGS	4500	2	64	Alaska-Huancayo.	10300	$1\frac{1}{4}$
1	Texas-Ottawa . .	2950	≤ 0.3	134	Alaska-Georget. .	5350	$1\frac{1}{4}$
6	Mexico-Ottawa . .	4200	12	158	Utah-Georgetown	3000	0.7
134	Alaska-Ottawa . .	4850	1.1	1	Texas-Georgetown	2600	0.4
134	Alaska-Halifax . .	5500	1.0	3	Mexico-Georget. .	3400	$1\frac{3}{4}$
134	Alaska-Saskatoon	2700	$\leq \frac{1}{2}$	156	Nevada-Georget. .	3550	2
158	Utah-Ottawa . .	3050	$\leq \frac{1}{3}$	124	Mexico-Harvard .	4050	3
163	Alaska-Huancayo.	10150	$\leq \frac{3}{4}$	134	Alaska-Harvard .	5300	1.0
11	Alaska-Little Rock	4900	3	64	Alaska-Technology	5400	1.2
134	Alaska-Little Rock	4900	2	23	New Foundland-Victoria	5000	2
134	Alaska-Florissant.	4600	2	144	Baffin Bay-Huancayo	9450	$\frac{2}{3}$
3	Mexico-Florissant.	2600	$\leq \frac{3}{4}$	158	Utah-Huancayo .	7100	0.6
11	Alaska-Florissant.	4650	1.3				
6	Mexico-Florissant.	2800	1.4 ?				

b) Reflections in South America.

Recorded at Huancayo (Peru) No.	Epicenter	Δ	PP/P	No.	Epicenter-station	Δ	PP/P
9	Nicaragua	2950	0.8	24	Colombia-La Paz .	2800	$\leq \frac{1}{2}$
5	Panama	2330	$1\frac{1}{2}$	37	Peru-La Plata . .	2700	0.4
35	Atlantic	6800	$1\frac{1}{3}$	27	Peru-La Plata . .	3800	0.7
165	Panama	2150	0.8	25	Ecuador-La Plata	4200	1.3
38	Atlantic	7300	0.4	24	Colombia-La Plata	5050	1.1
94	Atlantic	6700	0.6	40	Chile-La Plata . .	2000	0.5
167	Atlantic	6450	0.5	50	Chile-Rio de Jan.	3200	$1\frac{1}{2}$
122	Falkland Is. . . .	5000	3	49	Chile-Rio de Jan.	3050	0.8
168	Panama	2450	1.4 ?	25	Ecuador-Rio de J.	4550	2.1
178	Atlantic	5000	3	24	Colombia-Rio de Janeiro	4700	1.0

c) Reflections in Antarctica, epicenter South Atlantic (No. 94).

Station	Δ	PP/P	Station	Δ	PP/P
Wellington	8650	0.4	Melbourne	9100	ca. 1
Christchurch	8450	0.4	Perth	9150	$1\frac{1}{2}$
Adelaide	9350	0.7			

islands and submarine ridges in this part of the Pacific. For example, the reflection at 25° S. 85° W. is in the vicinity of the "Merriam Ridge" discovered by the CARNEGIE in 1929 [43]), which is probably connected with the islands of S. Felix and S. Ambrosio.

Table 10.
Observed values of PP/P, horizontal, from paths with reflections in the bottom of the Pacific Ocean.

a) Recorded at Pasadena.

No.	Region	Δ	PP/P	No.	Region	Δ	PP/P
12	Alaska	4000	1.3	59	Solomon Is. . . .	9800	0.7
13	Hawaii	4000	0.7	60	Solomon Is. . . .	10100	0.7
16	Aleutian Is. . . .	4400	0.8	61	Solomon Is. . . .	10150	0.5
115	Aleutian Is. . . .	4500	1.0	62	Solomon Is. . . .	10150	0.9
20	Aleutian Is. . . .	4800	1.0	63	Solomon Is. . . .	10000	0.8
21	Aleutian Is. . . .	4950	0.9	65	Bismarck Is.. . .	10300	0.8
26	Aleutian Is. . . .	5900	0.6	66	New Zealand . .	10350	0.8
29	Kamchatka . . .	6350	0.2	67	New Zealand . .	10500	1.2
30	E. Pacific	6500	0.2	119	New Zealand . .	10650	2.1
31	Kamchatka . . .	6600	$\leqq$ 0.4	74	New Guinea . . .	11200	4
34	E. Pacific	6800	$\leqq$ 0.4	77	Philippines . . .	11550	4 ½
36	Kamchatka . . .	7000	0.5	83	Philippines . . .	11950	10
37	Peru	7350	0.6	79	Philippines . . .	11600	3 ½
39	Kurile Is.	7550	1.0	85	Off Celebes . . .	12300	5
40	N. Chile.	7800	0.5	87	Banda Sea . . .	12550	12
116	Samoa	7900	0.6	88	Celebes Sea . . .	12700	10
117	Samoa	7900	0.5	121	New Hebrides . .	9700	0.8
41	N. Chile.	8100	0.8	123	Bismarck Is.. . .	10200	3.2
43	Japan.	8300	0.7	127	Samoa	8000	½
44	Japan.	8400	0.5	128	Bismarck Is.. . .	10450	0.4
45	Japan.	8350	0.4	129	Marianne Is. . .	9400	¾
47	Chile	8700	0.4	130	New Hebrides . .	9550	½
48	Chile	8700	0.3	131	Solomon Is. . . .	9600	1 ¼
49	Chile	8900	0.4	132	Solomon Is. . . .	9750	¼
50	Chile	9000	0.6	133	Philippines . . .	11800	5
51	Japan.	9000	0.8	135	Bismarck Is.. . .	10200	¾
118	New Hebrides . .	9250	0.6	145	Bismarck Is.. . .	10550	1
53	Marianne Is. . .	9330	$\leqq$ 0.3	147	Santa Cruz Is. . .	9400	1 ¼
52	N. of Marianne Is.	9300	$\leqq$ 0.8	148	Santa Cruz Is. . .	9450	1
54	Kermadec, Pacific	9400	0.5	149	Santa Cruz Is. . .	9400	0.6
55	Marianne Is. . .	9550	0.4	150	S. of Japan . . .	9900	1 ½
56	Tonga Is.	9650	0.7	152	Aleutian Is. . . .	4900	1
57	S. Japan	9650	0.6	182	SE. Pacific . . .	8100	$\leqq$ ¼
58	Solomon Is. . . .	9600	0.7				

Table 10 (continued). b) Recorded at Huancayo (Peru).

No.	Region	Δ	PP/P	No.	Region	Δ	PP/P
160	Samoa	10350	1	175	Lower California .	6450	0.7
33	California	6770	$\leq \frac{1}{2}$	176	Lower California .	6450	0.6
19	Mexico	4600	$\leq \frac{1}{2}$	154	Mexico	4750	0.8
15	Easter Is	4200	1.7	142	Mexico	4800	≤ 0.7
4	Galapagos Is. . .	2300	0.4	139	Guatemala . . .	3400	1
164	Mexico	4300	$1\frac{3}{4}$	180	Nicaragua	3050	≤ 1
6	Mexico	4600	0.3	126	Mexico	4200	0.8
124	Mexico	4500	0.6	119	New Zealand . .	10500	1.8

Table 11.
Observed values PP/P, horizontal, from paths with reflections in the bottom of the Pacific Ocean.

No.	Epicenter-station	Δ	PP/P	No.	Epicenter-station	Δ	PP/P
138	Alaska-Berkeley .	3120	$\leq \frac{1}{2}$	40	Chile-Wellington .	10400	≤ 0.6
134	Alaska-Berkeley .	3230	$1\frac{1}{4}$	48	Chile-Wellington .	9500	$\frac{3}{4}$
136	Alaska-Berkeley .	3290	0.9	49	Chile-Wellington .	9200	$1\frac{1}{2}$
11	Alaska-Honolulu .	4450	0.8 ?	40	Chile-Christchurch	10400	≤ 0.7
134	Alaska-Honolulu .	4550	0.7	152	Aleutian Is.-Berk.	4400	1.2
169	Mexico-Honolulu .	6400	0.4	34	Easter Is.-Berkeley	7100	≤ 0.4
170	Mexico-Honolulu .	5600	0.9	40	Chile-Berkeley . .	8400	0.6
171	Mexico-Honolulu .	5600	0.8	29	Kamchatka-Berk.	5800	≤ 0.3
172	Mexico-Honolulu .	5600	0.7	116	Apia-Berkeley . .	7700	0.4
112	Mexico-Honolulu .	5150	≤ 0.8	116	Apia-Victoria . .	8250	≤ 0.5
44	Japan-Honolulu .	5800	0.6	13	Hawaii-Berkeley .	4200	0.9

C. Atlantic reflections. Numerical data on reflections taking place in the Atlantic are given in Table 12. The seismograms were selected to give reflections in all parts of the Atlantic area, and at such distances as to give a clear discrimination between continental and Pacific types of reflection. All cases agree much better with the mean data for continental reflection than with those for Pacific reflection. This confirms the result already found from the velocities of surface waves, that the floor of the Atlantic Ocean is a region in which the surface layer has physical properties similar to those of the continental surface layer. The thickness of this layer cannot be determined from these data on reflections, but it must be at least a large fraction of the wave length, which is in most cases between 20 and 30 km.

D. Reflections in the Indian Ocean. Numerical data of this group are given in Table 13. Except for two points from seismo-

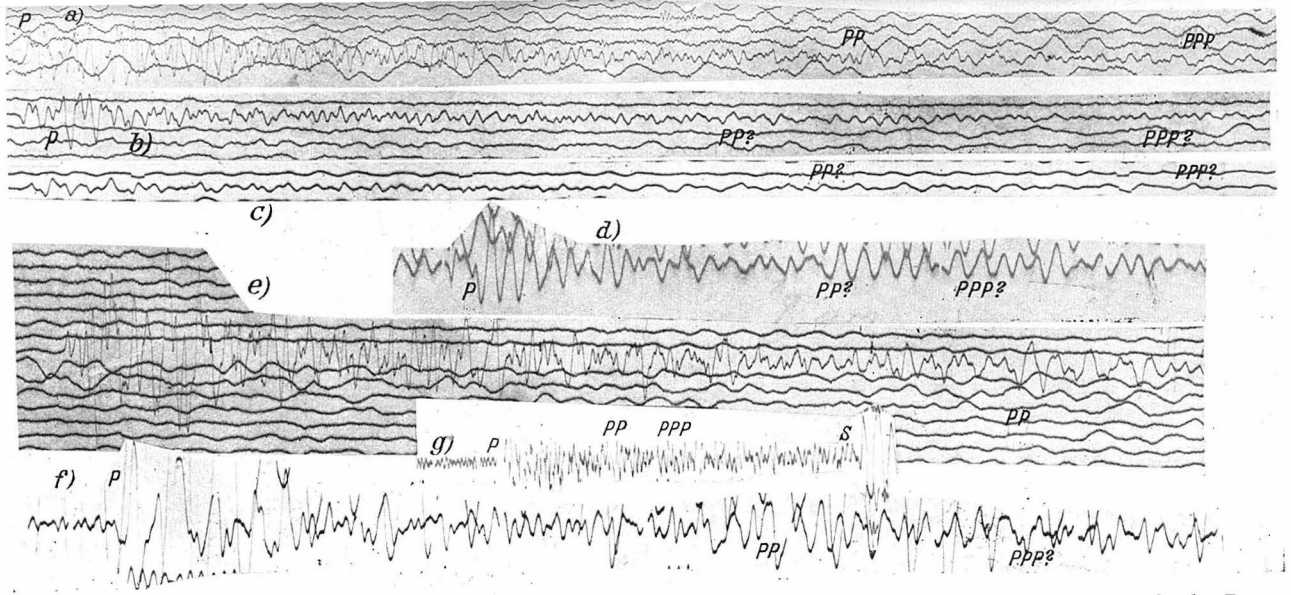

Fig. 8. Seismograms with reflections in the Pacific Ocean, showing small PP and PPP. (a) No. 29, Kamchatka-Pasadena NS, 57°; (b) No. 30, Easter Island-Pasadena Z, 58°; (c) No. 34, Easter Island Pasadena Z, 61°; (d) No. 29, Kamchatka-Berkeley Z, 52°; (e) No. 40, Chile-Pasadena Z, 70½°; (f) No. 40, Chile-Christchurch Z, 94°; (g) No. 169, Mexico-Honolulu EW, 58°.

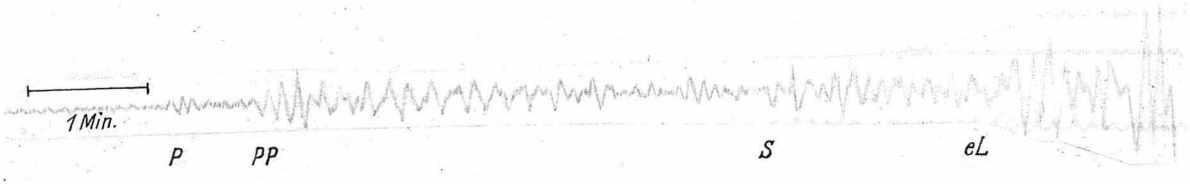

Fig. 9. No. 183, Galapagos-Huancayo EW, 31½°, showing large PP reflected in the Pacific Ocean.

grams of the Sumatra shocks, all these are from shocks occurring southeast of Madagascar, about 34° S. 57° E. In most cases the reflection is clearly of continental type, which supports the conclusion previously reached on scanty data from surface waves, that at least a large part of the floor of the Indian ocean is of continental (or Atlantic) character.

E. Reflections in the Arctic basin. Table 14 gives numerical data for reflections in the Arctic region. The last columns of this table give the approximate coördinates of the points of reflection. In all but four cases the ratio of amplitudes is so low as to fit the curve

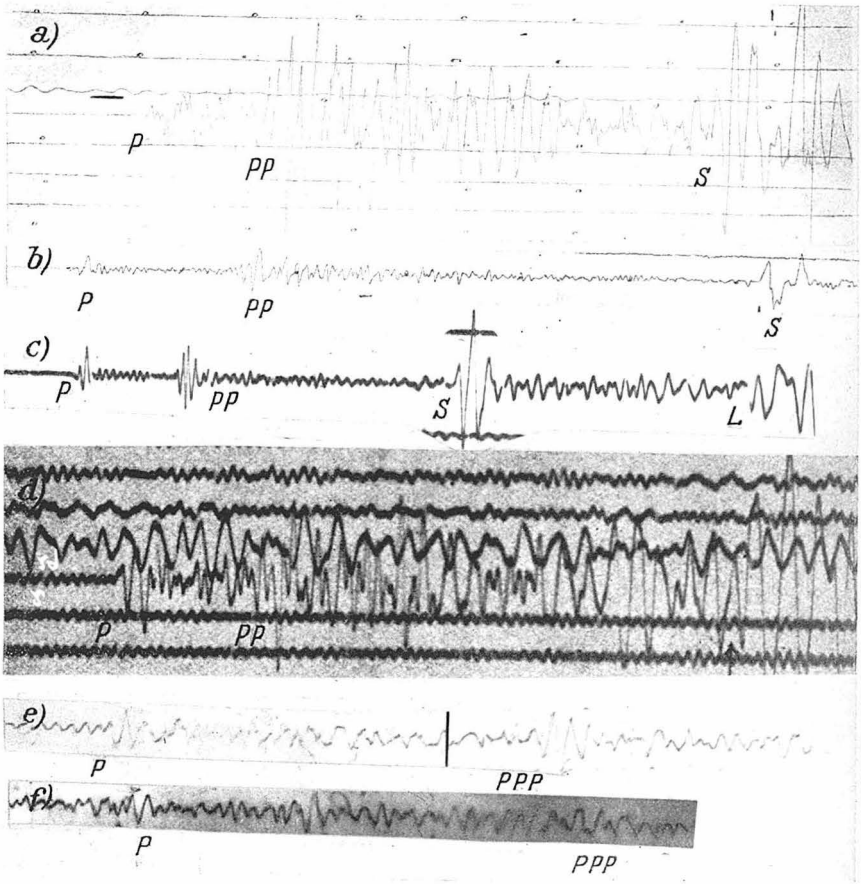

Fig. 10. Seismograms with epicentres and reflections in the Atlantic Ocean, showing large *PP* and *PPP*. (a) No. 94, La Plata NS, 33°; (b) No. 96, La Plata EW, 39½°; (c) No. 96, Rio de Janeiro NS, 41½°; (d) No. 46, Scoresby-Sund NS, 31½°; (e) No. 58, Huancayo NS, 58°; (f) No. 42, Scoresby-Sund NS, 60°.

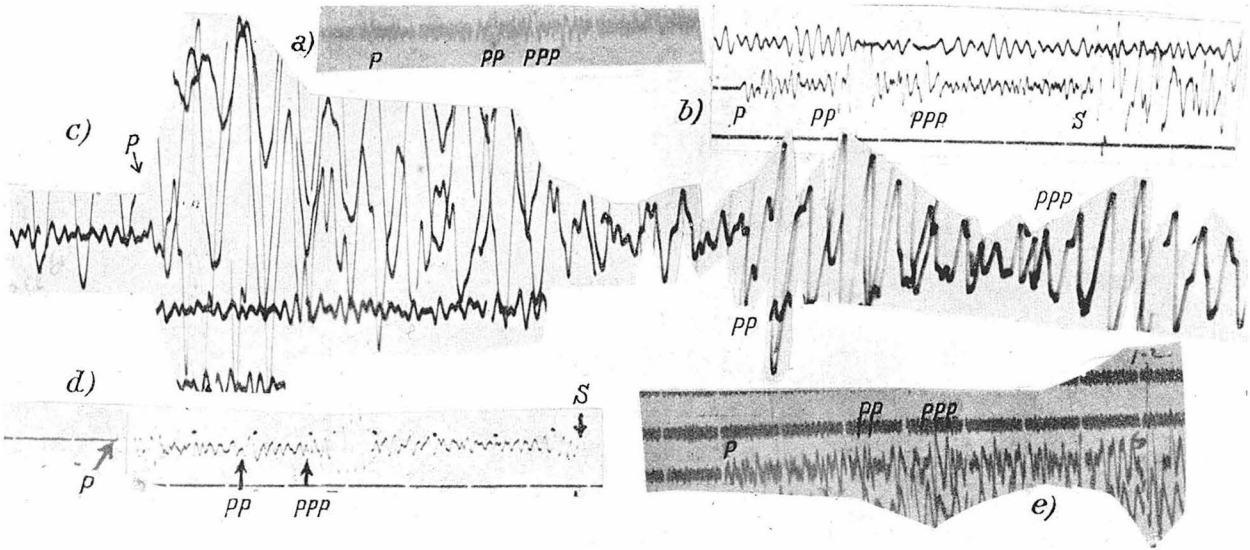

Fig. 11. Seismograms with reflections in the Indian Ocean, showing large *PP* and *PPP*. (b) from Sumatra shock of Sept. 25, 1931, at Bombay, NS, 38°. Other epicenters near 34° S. 57° E: (a) No. 106, Perth NS, 48½°; (c) No. 107, Christchurch Z, 84°; (d) No. 107, Bombay NS, 53½°; (e) No. 107, Perth NS, 49°.

Table 12. Observed values PP/P, horizontal, with origins and points of reflection in the bottom of the Atlantic Ocean.

No.	Station	Δ	PP/P	No.	Station	Δ	PP/P
42	Scoresby Sund . .	6700	1.3	94	La Plata	3650	$2\frac{1}{2}$
46	Scoresby Sund . .	3500	1.9	95	La Plata	4200	4
35	Technology . . .	7350	0.8	96	La Plata	4400	$2\frac{1}{2}$
76	Georgetown . . .	7900	1.2	94	Rio de Janeiro .	4250	1.1
32	Harvard	3000	0.5	95	Rio de Janeiro. .	4800	1.4
35	San Juan	6220	0.7	96	Rio de Janeiro. .	4600	1.4
46	San Juan	5230	1.3				

Table 13. Observed values PP/P, horizontal, with points of reflection in the bottom of the Indian Ocean. The first two shocks originated of Sumatra the others SE of Madagascar.

No.	Station	Δ	PP/P	No.	Station	Δ	PP/P
	Bombay	4200	2.5	107	Amboina	8000	1
	Tananarive . . .	6150	0.8	107	Medan	6000	1.2
106	Wellington . . .	9500	0.7	107	Batavia	5900	1.4
107	Wellington . . .	9500	0.5	108	Batavia	5900	1.0
107	Melbourne	7600	1	108	Medan	6000	$1\frac{1}{4}$
107	Christchurch . . .	9200	0.8	107	Colombo	5100	1.0
106	Perth	5400	1.3	107	Bombay	5950	1.2
107	Perth	5400	1.2	108	Bombay	5950	0.6
106	Batavia	5950	1.2	107	Adelaide	7200	1.2

Table 14.

Observed values PP/P, horizontal, with points of reflection in the Arctic region. Epicenters in Alaska. The first two seismograms show PP reflected at continental structure; values of PP/P which correspond to continental reflection of PP are marked by *.

No.	Station	Δ	PP/P	Reflection at N. lat.	Reflection at W. lg.	No.	Station	Δ	PP/P	Reflection at N. lat.	Reflection at W. lg.
134	Scoresby S.	5000	1.3*	78	105	134	Abisko . .	5650	0.5	86	115
185	København.	7100	0.5*	81	55	185	Upsala . .	6800	≤ 0.3	$82\frac{1}{2}$	65
185	Leningrad .	6900	0.8*	86	75	185	Helsingfors .	6850	small	84	65
185	Pulkovo . .	6900	0.6*	86	75	138	Abisko . .	5900	<0.6	$84\frac{1}{2}$	135
134	Upsala . .	6550	0.27	86	50	136	Abisko . .	6200	0.5	83	150
136	Upsala . .	7150	0.2	$87\frac{1}{2}$	120	134	Helsingfors .	6400	0.3	88	45
138	Upsala . .	6800	≤ 0.3	87	85	136	Helsingfors .	7150	0.2	$87\frac{1}{2}$	160
138	Helsingfors .	6800	0.15	89	130						

for Pacific reflection. (See Fig. 12.) In two of these four cases the reflection is within the North American continental area, and the re-

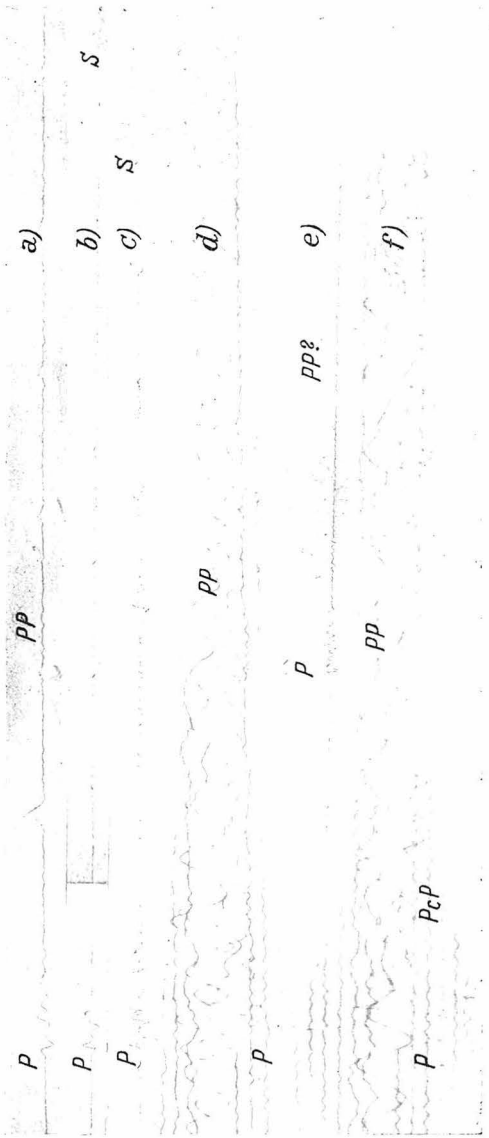

Fig. 12. Seismograms with reflections in the Arctic basin, showing small *PP*. Epicenters in Alaska. (a) No. 136, Helsingfors NS. 64½°; (b) No. 136, Upsala NS. 64½°; (c) No. 134, Upsala NS. 58°; (d) No. 136, Abisko NS. 56°; (e) No. 134, Helsingfors Z. 57½°; (f) No. 136, Abisko Z. 56°.

flections are clearly of continental type. Less easily accounted for are the remaining two instances — seismograms at Leningrad and

Pulkovo, reproduced by SOMMER[2]). These are also of continental type, but the reflections are within the Arctic basin, near other points where the reflection is "Pacific".

The small PP cannot be an effect of crustal structure near the stations, since the same stations record continental PP from other epicenters. Nor is it likely that it is due to an azimuthal distribution of energy connected with the mechanism of the shocks, as continental and "Pacific" reflections occur in nearly the same azimuth, and about at the same distance. Moreover, it would require a very special mechanism to affect P and PP in different ways.

It is noteworthy that it is possible to delimit a closed area which contains all the points of reflection for the small PP. This area coincides with the deepest known part of the Arctic basin, so that it is possible that in this region the continental layer is either very thin, or altogether absent.

F. Special and exceptional cases. In addition to the groups discussed above, a few particular instances deserve special mention. As was to be expected, reflections in Hudson's Bay (shock number 143, at Pasadena) and the Gulf of Mexico (number 24, at Pasadena) show continental character. On the other hand, all three Panama shocks (nos. 18, 140, 141) show the unusually small ratio 0.4 for PP/P at Pasadena, distant about 4600 km., although the point of reflection is at about $22^1/_2°$ N. $98^1/_2°$ W., near Tampico, Mexico. As may be seen from Fig. 6, these points if plotted would fall on the sharp discontinuity of amplitudes, and would extend it to lower values.

In favorable cases there is a possibility of using the ratio PP/P to trace the boundary between regions of continental and Pacific structure. For example, the Pasadena seismograms of shocks numbers 25 and 28, with points of reflection near 15° N. 98° W., show Pacific reflection; while number 27, with reflection near 15° N. $96^1/_2°$ W., shows continental PP/P. The former point is in the Acapulco Deep, while the latter may be on the continental shelf.

At Pasadena, shocks from the Aleutian Islands and the western part of Alaska regularly give Pacific reflections; but shocks farther east give continental PP/P. Such shocks are numbers 11, 134, 136, 138, 151, with reflections at 47° to 49° N. and 129° to 134° W. Shock number 137, with point of reflection at 48° N. $130^1/_2°$ W., appears to show a Pacific type reflection; but the seismograms of this shock are peculiar, and there is some evidence of depth slightly greater than normal.

VIII. Other amplitude ratios.

A. PPP/P. PPP waves with points of reflection in the continental areas or the Atlantic or Indian Ocean (see Fig. 11) begin to be clearly visible on the seismograms beginning at distances of about 5000 km. The amplitude ratio PPP/P in these cases scatters about 1 up to distances of about 7200 km. Near 7500 km. most values of this ratio are somewhat larger than 1; since PP/P is also large about 7500 km., this is presumably due to small amplitudes of P. Between 8000 and 9300 km. PPP/P is somewhat less than 1.

PPP/P for cases of Pacific reflection is almost invariably small (see Fig. 8), so that PPP is rarely observed at Pasadena. Two observations of PPP/P for Arctic reflection show values which are about half the normal for continental reflection, while in other cases of the same kind PPP is not to be found (Fig. 12).

All observations on PPP/P are consistent with the conclusions drawn from PP/P.

B. PP/P'. Between 11000 km. and 15500 km. (100° and 140°) PP is larger, occasionally very much larger, than P'. Even for PP/P the result depends somewhat on the constants of the instruments used, as PP is usually longer in period than P. For PP/P' this becomes more serious, as at large distance the periods of PP become very long, while those of P' (especially the diffracted P') are very short. Beyond 140° PP/P' decreases rapidly, with a very small minimum (absolute minimum 0.05) corresponding to the large amplitudes of P' near the focus, at distances of 143°—147°. At larger distances PP becomes larger than P' in the horizontal components, and about equal to P' in the vertical component.

C. Amplitudes of SS. S may be considered composed of the two components SV and SH, polarized respectively in the plane of propagation and normal to it. The latter is always totally reflected at the surface of the earth, so that SS originating in this way should show the same behaviour as S at half the distance. SV is totally reflected up to distances of about 25°; so that up to 50° SS should show no loss of energy due to reflection. From 50° on, SS originating from SV shows the same behaviour as PP at shorter distances. From 75° to 100° this SS wave should show very small amplitudes, as only a small fraction of the SV energy goes into the reflected SS, most of it going into SP. With increasing distance a larger fraction of the SV energy is reflected as SS, this fraction being larger for continental than for Pacific reflec-

tions. It is difficult to compare observation with theory, as the two polarizations are superposed; the vertical component should show only the *SS* originating from *SV*, but this is usually rather small.

D. Amplitudes of *PS*, *PPS* and *SKSP*. The observed *PS* also includes *SP*, which cannot readily be separated for normal shocks. For zero focal depth the percentage of energy going into the transformed wave arriving at a given distance is the same for *PS* and *SP* [9]), so that any difference in energy of *PS* and *SP* must then be attributed to a difference in the original energy of *P* and *S*. At the beginning of the *PS* curve, where it branches from *S* (at about 50°), the amplitudes must be very small, since very little energy is reflected into these waves; but the percentage of transformed energy increases very rapidly with distance, and between 70° and 100° *PS* (or *SP*) carries more than 90% of original *P* (or *S*) energy. As both *P* and *S* have large amplitudes near the corresponding points of reflection, *PS* is a large wave in the whole range mentioned. Beyond this the percentage of energy going into the transformed wave decreases slowly with distance; but even at the end of the *PS* curve (between 130° and 140°), where the transverse part of the path becomes tangent to the core, this fraction is still over 70%, so that *PS* is a large phase to the end of the range of observations.

Similar considerations apply to the *PPS* group of waves; in this case it is *PSP* which carries a very large fraction of the original energy. This is confirmed by the observation of *PPS* as a large wave at large epicentral distances. Similarly *SKSP* should carry much of the energy of the original *SKS* (and *P* in *PSKS* or *S* in *SPKS*); this is well observed under similar circumstances.

IX. Appearance of normal seismograms at various distances.

The following general remarks are presented with a view to facilitating the determination of epicentral distance from the seismograms of a single station, and the identification of the phases recorded. Consequently, the description refers chiefly to the larger and more conspicuous phases, with the addition of a few which are not large, but are very useful in the determination of distance. It is based primarily on the seismograms at Pasadena and Huancayo. Experience with seismograms lent by other stations, or reproduced in the literature, makes it possible to write a description which will be fairly general in application. Some differences exist, due to differences in instrumental con-

stants or to the Pacific situation of Pasadena and Huancayo; these will be pointed out. Of the latter group, the most important are the variation in amplitude of PP and PPP at certain distances, depending on whether the reflection is in a region of continental or Pacific structure (see sections VII and VIII); and the considerable decrease in the amplitudes of surface waves which have traversed regions of complicated crustal structure.

The description of course applies to shocks at normal depth. Before assigning a distance from any seismograms it is necessary to be positive whether one is dealing with a case of deep focus. Presence or absence of surface waves is not a sufficient criterion for this purpose. As just mentioned, normal shocks occasionally record with small surface waves, which have lost energy due to absorption or scattering along a complicated path. On the other hand, deep-focus shocks of considerable energy appear to produce some true surface waves, and also a complicated series of long-period reflected bodily waves, which may have the appearance of surface waves. It is necessary in all cases to search carefully for such phases as pP, sP, etc.

The appearance of the seismogram depends very much on the characteristics of the instrument. Vertical instruments with short period and high magnification, such as are in service at Pasadena, record important phases such as $PKKP$ and $P'P'$ which are otherwise not observed. Long period instruments are desirable for good records of certain phases which regularly record with long periods, especially at large distances, such as PS, PPS, SS, SSS, $SKSP$, G. In general the appearance of the vertical-component seismogram will differ very much from that of the horizontal. Especially at large distances, the various longitudinal waves often have high angles of emergence, and are accordingly well registered only in the vertical component; while phases consisting chiefly of transverse waves under similar circumstances are frequently polarized in such a way that they are found only on the horizontal-component seismograms. In general, if only one seismogram is to be available it should be in the vertical component, as the appearance of the record then does not depend on azimuth, and the initial phases (P, P') are well registered.

In determining the distance of a recorded shock, the first step should be to ascertain the time interval between the beginning of the seismogram and the registration of the first long waves and of the maximum. This gives at once a rough approximation to the true distance,

which is less subject to errors of interpretation than any other method. It should be considered that the beginning of the surface waves cannot be earlier than the time given as that of G in the chart at the end of our first paper. (This was drawn for a velocity of 4.45 km./sec.) If the period of the first surface waves is much less than one minute, eL should be noticeably later than the expected time for G. Vertical instruments usually record the beginning of the Rayleigh waves, which is still later. Care is required not to identify SS and SSS as eL. Especially in the case of SS, large errors may result. However, SS is usually recognizable as a single large wave, which is not immediately followed by a wave train or by a building up of waves to the maximum.

Judging by published bulletins, the most frequent errors in the interpretation of seismograms at the present time are the following:

(1) At distances of about 115° to 120°, PP and PS are identified as P and S, so that the distance is taken to be about 80°. This can be avoided by the precaution just discussed, as at 115° the surface waves arrive very much later than at 80°.

(2) From 84° onwards, SKS is misidentified as S. As soon as the measured $S—P$ exceeds $10^m\ 15^s$, there is a considerable possibility of this error. Attention should be directed to the appearance of the entire S group of phases (including SKS, S, PS, etc.), which is discussed in detail below.

(3) In cases of deep focus, pP or some similar phase may be identified as S, with the result that the shock is assigned too short a distance, or even reported as a local shock.

For the first six degrees normal seismograms have the characteristics for "local" shocks; P and S show complications due to the local structure, and the maximum follows immediately upon the S group.

From 7° to 12° there are usually no clear phases between P and the beginning of surface waves (Fig. 14). In many cases there is a large long-period iL with short periods superposed. Certain seismograms between $8^1/_2°$ and 9° show a rather large short-period iS (Fig. 15). Intermediate instances occur, in which the short periods of the S group obscure the beginning of surface waves, but do not display any clear phases. For further details see section X.

From 13° to 26° there are usually clear iP and iS (Fig. 3). P frequently shows multiplicity. Between 18° and 22° iS is almost always a large wave of period between 10^s and 20^s. From 22° to 26° S

often has the same character, but there are a number of cases where there is an indefinite *eS*.

From 26° to 37° *P* and *S* are usually clear (Fig. 5b—e). *S* is usually larger in the horizontal components than in the vertical, and shows long periods toward the end of this range. *PP* is clear in cases of continental reflection. *PcP* (see Fig. 2), *PcS*, and *ScS* are frequently recorded, and often large. (See Fig. 10 of the first paper, on page 120.)

From 38° for a few degrees *P* is small, but increases again immediately. For the whole range from 40° to 84° the beginnings of both *P* and *S* are usually quite clear, so that *S*—*P* as read from seismograms in this range is usually reliable; its value then ranges from about $6^m\ 10^s$ to $10^m\ 15^s$. Other values of *S*—*P* require critical examination before use in locating epicenters.

In this range *P* frequently shows multiplicity; the No. 2 of our first paper, which usually follows after 15 to 17 seconds, is often large and might possibly be taken as the beginning. *S* often shows long periods (15—20 seconds, or even more). With short-period instruments this may result in very small recorded amplitudes. The longer periods prevail from 40° up to about 55°, beyond which both short and long periods are usually recorded. Between 40° and 84° *S* shows all types of polarisations[24,9]) with *SV* probably prevailing.

PP is very large from about 38° to 75°, especially in cases of continental reflection. *PPP* begins to be evident at about 40°.

Between 40° and 60° *PcS* often appears preceding *S*. *ScS* and *SS* are occasionally well recorded between 40° and 84°.

The phase *P'P'*, which has been reported by the authors[25]), appears chiefly between 55° and 90°. In this range it affords a valuable check on the distance, as the interval *P'P'*—*P* varies rapidly with distance and is nearly independent of depth. *P'P'* is found only on the seismograms of short-period vertical instruments.

Even in the range which we have been discussing, where the seismograms are in general simple in character and easy to interpret, there are exceptional instances. Especially shocks in particular regions may give peculiar records at a particular station or group of stations. For example, shocks in the region of Samoa are usually recorded at Pasadena (distant about 71°) with a large *P*, large *L*, and practically no *S*. Yet South American shocks at about the same distance from Pasadena are recorded there with a large *S*; and the Samoan shocks record with a conspicuous *S* at Berkeley, which is less than half a degree nearer.

It is noteworthy that shocks in the region of the New Hebrides (near 13° S. 167° E.) appear to occasion exceptional difficulty at most stations. The location of epicenters in that district is correspondingly troublesome. This is not merely an accident of location with respect to the stations; it appears to be due to the mechanism of the shocks themselves, which results in the *S* group being generally weak.

A somewhat similar case is that of the aftershocks of the Baffin Bay earthquake of November 20, 1933. At Pasadena, these shocks, especially that of December 19, 1933 at 17^h, show practically no *S*, and record peculiar short periods immediately preceding the large surface waves. Judging by the bulletins of other stations, there has been general difficulty with the seismograms of these aftershocks.

It is very much to be desired that such exceptional cases should not escape attention. Many stations make a practice of indicating in their bulletins those shocks which give exceptional or peculiar seismograms.

The seismograms at distances from 84° to 103° form a group of much the same general character. It is usually quite easy to recognize that a given seismogram belongs in this range of distance; but to decide the precise distance within the range is often much more difficult. *P* is usually clear, and is followed after between ten and eleven minutes by the complicated *S* group of waves, which includes *SKS*, *S*, *PS*, and some other less well defined phases.

P is not very large in this range, but is usually well recorded; in the latter half of the range the amplitudes are sometimes rather small, and as in these cases there is usually a large *PP* about four minutes later, small seismograms may appear to begin with *PP*. *P* shows much multiplicity. *PPP* is occasionally conspicuous (for continental reflections).

From 84° to 90° the *S* group is usually not very clear. It begins with *SKS*, which is very small and is usually observed in this range only in large shocks. This is immediately followed by a larger *S*, which usually has a rather indefinite emergent beginning. The disturbance continues after *S*, and occasionally *PS* is distinguishable as a long-period wave about one minute following *S*.

Beyond 90° *SKS* increases very rapidly; it is already large at 93°, and continues so beyond the range here considered (for its behaviour beyond 103° see the remarks below). It regularly shows the polarization required by theory; that is, it is well recorded in the vertical and the longitudinal horizontal components, but is absent from the transverse horizontal component.

S continues large through this whole range; it usually has a sharp beginning (iS); it is very large in the few degrees about 95°, but beginning about 99° it decreases with distance. The polarization may be opposite to that of SKS; in the European records of the Sumatra shocks S is recorded chiefly in the horizontal transverse component (SH). This seems not be general, and the sharp polarisation appears to depend on the mechanism of the shock. PS shows the same polarization as SKS. It is a large phase, usually with long periods, in this interval, and appears to increase slowly with distance. SS is sometimes very large, but appears to be recorded irregularly. Theoretically the amplitude should be much affected by polarization, as SH is totally reflected, while SV should lose most of its energy when reflected at distances giving SS in the range here considered, most of the energy being transformed into longitudinal waves.

Short-period vertical instruments begin to record $PKKP$ at about 95°. $PKKP—P$ affords a valuable check on the distance, as this interval increases rapidly with distance (and does not depend on depth of focus).

The shadow zone for P begins at about 105°. This distance separates the simpler seismograms, recorded at small to moderate distances, from the very complicated seismograms characteristic of large distances. The amplitude of P here falls off very rapidly with increasing distance, and the direct P waves are replaced by longer period diffracted P waves. These diffracted waves, which occur within the shadow zone, are recorded at distances beyond 105°, only in large shocks, and only on vertical instruments with high magnification for long periods. There is a similar phenomenon for S waves, but the diffracted S appears to be recorded more frequently than the diffracted P. Both phases show multiplicity, and the earlier phases of both groups appear to fade out at large distances, where only the later waves are recorded.

From about 105° to 128°, the first large phase of the seismogram is PP. It is preceded by the "diffracted" P'; this is not a large phase, but is sometimes very conspicuous on the records of short-period vertical instruments. When the shock is large enough so that this phase is recorded, the interval $PP—P'$ is valuable in determining the distance. The same remarks apply to $PKKP$ and the interval $PKKP—P'$ (or $PKKP—P$). PPP is a large phase when the reflections are continental.

SKS is large about 105°, and decreases somewhat with distance. PS is usually very large; other conspicuous phases are PPS, SS, and SSS.

The next range of distance, 129° to 141°, is characterized by the

presence of *SKP* (or *PKS*); this is usually the largest phase in the preliminary part of the seismogram, as it has a focus about 131°—132°, and continues large for about ten degrees beyond. It usually shows much multiplicity.

In this range the "diffracted" P' is usually well recorded, especially on vertical instruments; but it appears to decrease with increasing distance. *PP* is regularly recorded, and may appear as a large phase between P' and *SKP*. In the first few degrees *PP*, *PS*, and *PPS* are often observed; but from 135° to 140° there are usually no definite phases between *SKP* and *SS*, which is large in this range. There are some observations of *SSS*.

At about 142° the focus of P' occurs. Approaching this point, the amplitudes increase very abruptly from the small "diffracted" waves to the large direct P'. With increasing distance P' at first presents an appearance of complication, and then separates into P_1' and P_2', both of which show multiplicity.

Also near 142°, *SKP*, which is decreasing with distance, is finally obscured by *PP*, and is not observed at larger distances where it should precede *PP*. *PP* continues to be observed regularly, and is large approaching 180°.

From 141° on, there are frequent clear cases of *SKKS*, *SKSP*, and *PPS*; they begin to be less clear approaching 160°. The seismograms near this latter distance often have an appearance of continuous and complicated motion without definite phases. *SS*, and even *SSS*, are often very large.

At distances approaching 180° the interval between the preliminaries and the surface waves is so large that the seismogram appears like a record of two separate disturbances. It begins with large P_1' and P_2' groups, followed by a large *PP*, and frequently with a clear *PP* over the larger arc. *PcPP'* and *PPP* are also large, and there is a large wave which arrives at the time calculated for *SKKKS*. There are very many other minor phases.

X. *P* and *S* at short distances. The problem of discontinuities in the mantle of the earth.

There is a well-known difficulty in interpreting the observations of *P* between 15° and 25°. The apparent surface velocity increases rapidly in this interval; investigators are not yet agreed whether this increase is continuous or not. If discontinuous, the effect should pre-

sumably be due to one or more discontinuities within the mantle, at depths of a few hundred kilometers. In this case, the travel time curve should consist of a series of intersecting straight lines, with no large change in amplitude at the points of intersection. If the increase in apparent surface velocity is continuous, the simplest hypothesis is that the velocity is nearly constant in the upper mantle to a depth of roughly 80 kilometers, where it begins to increase with increasing depth. The travel time curve should be nearly rectilinear up to a certain critical distance, and then curve gradually, with a sudden increase in amplitude at the critical point.

The increase of apparent velocity with distance was known to MILNE and others very early in the history of seismology; the matter was discussed with reference to possible discontinuities at depths of a few hundred kilometers by MILNE[26]), LASKA[27]), and BENNDORF[28]), but as their data were imperfect the conclusions cannot be compared with those of more recent investigators. The first valid discussion (1916) appears to be that of S. MOHOROVIČIĆ[29]), using the data of A. MOHOROVIČIĆ[30]). Within the mantle he finds in general a continuous increase in velocity with depth. At about 120 km. depth he finds a discontinuity of the second order, at which the velocity begins to increase more rapidly; the corresponding ray emerges at about 11°. At about 400 km. he finds another possible discontinuity, where the velocity may decrease by about 0.2 km./sec; the corresponding distance is about 23°. GALITZIN[31]) and WILIP[32]) attempted to establish such discontinuities from the observed angles of emergence. In 1926 GUTENBERG[33]) pointed out the occurrence of an abrupt increase in the amplitude of P at about 15°, as shown by the records of three earthquakes in Europe and one in Japan. This he interpreted as evidence of a sharp increase in the velocity at a depth of about 70 km. No other indication of discontinuities in the mantle was found.

In the same year BYERLY published a study of the Montana earthquake of 1925[4]) in which it is shown that the travel time curve for P shows an abrupt change of slope at about 20°, corresponding to a ray having its lowest point at a depth of about 400 km.

In 1931 the authors published a paper [34]) using the data of three strong Mexican shocks as recorded in California, and finding no sign of any discontinuity at depths between 40 and 500 kilometers.

In 1933 NEUMANN[35]) interpreted the travel time curve of the P waves of the Santiago de Cuba shock of 1932 as a series of straight

lines; the first pair of these intersect at 2100 km. (19°), corresponding to a discontinuity at a depth near 400 km., probably less. Intersections are also indicated at 3100 km. (28°) and 5500 km. (50°). He has recently[36]) applied the same interpretation to other shocks.

In 1934 Byerly[3]) found that the travel time curve of the Texas earthquake of 1931 shows a definite break near 16°, which he interprets as indicating a first-order discontinuity at a depth of about 300 km. Another break in the curve at 25° is strongly suggested. In discussing the Nevada shock of 1932[37]) he finds evidence of a sudden change in slope of the curve at about 28°, and of a very different slope from 4° to 12°, but he states that definite evidence of overlapping of the branches is lacking, and draws no conclusion as to discontinuities in the upper part of the mantle.

There is an unavoidable element of personal judgment in discussing the form and slope of travel time curves on the basis of observations which necessarily show a considerable scatter in any case. To reduce this element as far as possible, in his paper on the P waves of the Long Beach earthquake, Gutenberg[38]) used the apparent velocities between pairs of stations at distances two or three degrees apart, so far as practicable. These apparent velocities were then plotted against the corresponding mean distances. If for any range of distance the true travel time curve is rectilinear, the apparent velocity should be constant, and the corresponding points of the plot should cluster about a line parallel to the axis of distances. This proves to be the case up to 12°; beyond this the plotted points fall near a smooth curve. There is no evidence of a discontinuity; the data thus confirm the results of Gutenberg and Richter[34]).

A very careful and detailed discussion of the whole problem is given by I. Lehmann[39]). The data used are chiefly those of the Iceland shock of 1929 July 23 and the Atlantic shock of 1931 May 20. Both travel times and amplitudes are studied; but no positive decision is reached as to whether the unquestionable changes in apparent velocity and amplitude about 19° are due to a discontinuity. If real, this discontinuity is concluded to be at a depth between 250 and 300 km., but cannot be specified more precisely. The author is at pains to point out that, while the travel time curve can be represented by two or more straight lines, the observations are also consistent with a smooth curve. The amplitude relationships are found to be very complex, and difficult to interpret on any simple hypothesis.

It is evident that any further progress in this investigation calls for thorough discussion of a large body of data. Besides the travel times published by other investigators, we have available the readings of the Long Beach earthquake, and also those of a number of shocks in Mexico, Central America, and Alaska, as recorded at California stations.

The Long Beach travel times have the advantage that the epicenter and origin time are unusually well determined. The other shocks mentioned are so located that the stations in California are all in nearly the same azimuth, so that small errors in the epicenter do not appreciably affect the apparent velocities, although the mean distances between pairs of stations are of course somewhat uncertain. The stations used have good time corrections, similar instruments, and high-speed recording (60 mm./min.). The range in distance available is about $6^1/_2°$ (between Berkeley and La Jolla).

These data, as well as the travel times reported for various shocks by other investigators, have been handled by the method used in the paper by GUTENBERG on the Long Beach earthquake[38]), where the numerical data for that shock and three Mexican shocks may be found. The remaining data from California stations appear in Table 15 of the present paper. All the apparent velocities are plotted in Figure 13. The upper half of this figure shows the data of the Long Beach and Mexican shocks; the lower half shows points computed from the data given by BYERLY for the Montana and Texas shocks[3, 4]) and by LEHMANN for the Iceland and Azores shocks[39]). For these latter points numerical data are not tabulated here; they are derived from the published travel times and distances.

In studying this figure due attention should be paid to the large vertical scale; the variations in calculated apparent velocity at any given distance are really surprisingly small, as where δt is 20 seconds, altering it by one second changes the apparent velocity by five percent, or about $^1/_2$ km./sec. The distances are given in degrees and tenths; in calculation distances in kilometers were used. The full lines in the two sections of the figure are drawn to fit the corresponding points; the dashed line in the lower section is identical with the full line in the upper section, and it will be observed that the difference is not significant. Taking the whole body of data together, there is no evidence of a clustering of points at any particular apparent velocity, or at a series of definite apparent velocities; consequently there is no reason to draw

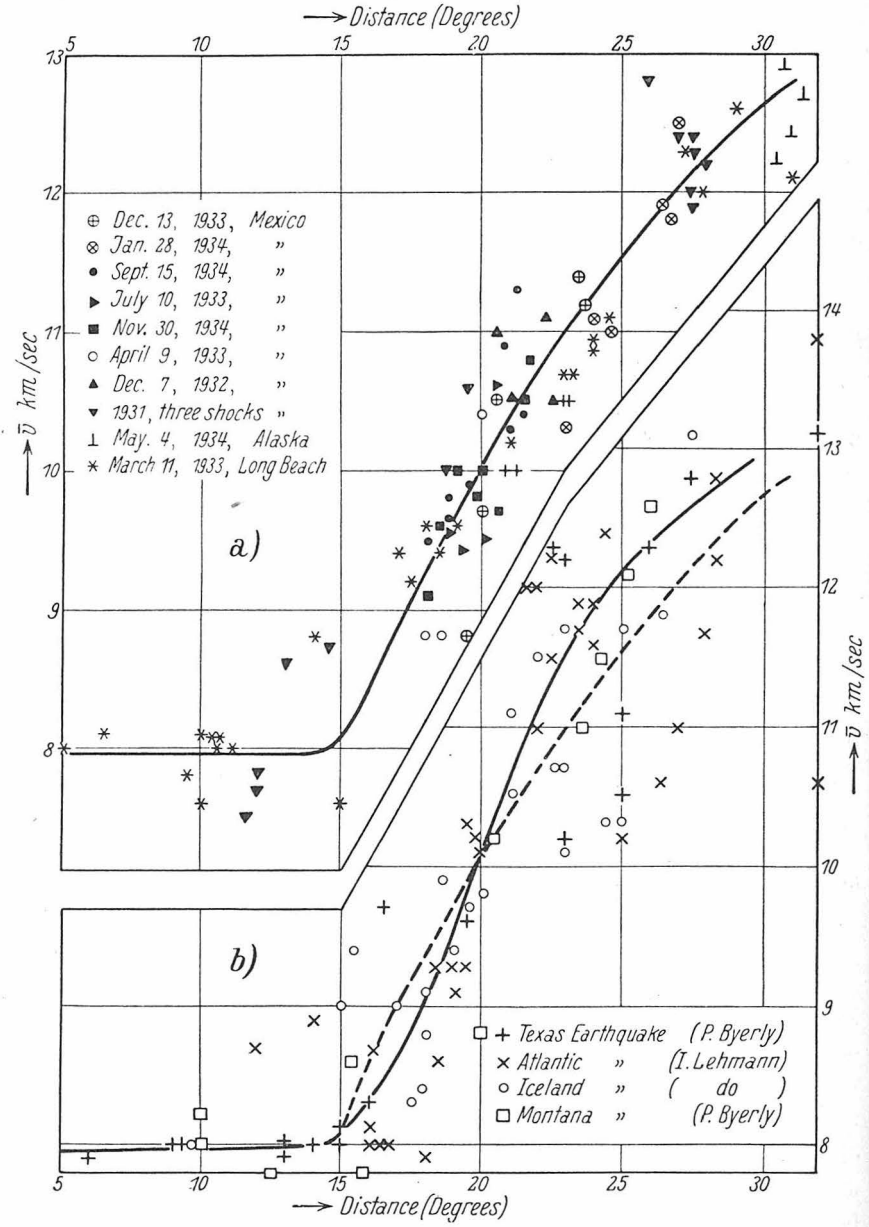

Fig. 13. Apparent velocity of P waves as a function of distance.

the curve as a series of steps, which would correspond to a travel time curve consisting of straight lines. The result therefore is in favor of gradual increase of velocity with depth, and not a discontinuous one.

Data on the amplitudes of P from 10° to 30° are scanty. In 1926 GUTENBERG[33]) found from the data of three European shocks and one in Japan that the amplitudes of P decrease with increasing distance to about 15°, where there is a large and abrupt increase; the amplitudes continue relatively large up to about 22°, then decreasing gradually.

Table 15.
Apparent velocity $\overline{v}$ of P as calculated from differences δt in times of arrival at stations a few degrees apart.

Station 1	Station 2	Distances ° °	δt sec.	$\overline{v}$ km./sec.
a) December 7, 1932, $16^h\ 22^m\ 09^s$, Mexico.				
La Jolla	Pasadena	19.6 21.2	15	11.0
Pasadena	Tinemaha	21.2 23.6	25	10.5
Santa Barbara	Tinemaha	22.3 23.6	13	11.1
La Jolla	Santa Barbara	19.6 22.3	27	10.5
b) April 9, 1933, $03^h\ 58^m\ 08^s$, Off Mexico.				
La Jolla	Pasadena	17.3 18.8	19	8.8
Pasadena	Tinemaha	18.8 21.3	27	10.4
La Jolla	Santa Barbara	17.3 19.8	32	8.8
c) December 13, 1933, $21^h\ 23^m\ 39^s$, Mexico.				
La Jolla	Pasadena	18.8 20.2	17	8.8
Riverside	Haiwee	19.6 21.6	21	10.5
Pasadena	Tinemaha	20.2 22.5	26	10.0
Pasadena	Haiwee	20.2 21.6	16	10.0
La Jolla	Santa Barbara	18.8 21.3	29	9.7
Santa Barbara	Berkeley	21.3 25.1	40	10.5
Tinemaha	Berkeley	22.5 25.1	26	11.2
Santa Barbara	Lick	21.3 24.4	32 ½	10.5
Tinemaha	Lick	22.5 24.4	18 ½	11.4
d) July 10, 1933, $03^h\ 21^m\ 38^s$, Mexico.				
La Jolla	Pasadena	17.9 19.4	17	9.6
Pasadena	Tinemaha	19.4 21.8	25	10.6
Pasadena	Haiwee	19.4 20.9	17	9.5
La Jolla	Santa Barbara	17.9 20.5	30	9.4

Table 15 (Continued).

Station 1	Station 2	Distances °	°	δt sec.	v km./sec.
e) January 28, 1934, $19^h\ 10^m\ 04^s$, Mexico.					
La Jolla	Pasadena	22.4	23.8	14 ½	10.3
Riverside	Santa Barbara	23.2	25.0	18	11.1
Pasadena	Tinemaha	23.8	25.7	20	11.0
Tinemaha	Berkeley	25.7	28.6	26	12.3
Santa Barbara	Berkeley	25.0	28.6	34	11.8
Tinemaha	Stanford	25.7	28.4	24	12.5
Santa Barbara	Stanford	25.0	28.4	32	11.9
f) May 4, 1934, $04^h\ 36^m\ 02^s$, Alaska.					
Berkeley	Haiwee	29.1	32.1	27	12.2
Stanford	Haiwee	29.4	32.1	23	12.9
Lick	Haiwee	29.7	32.1	21	12.4
Berkeley	Pasadena	29.1	33.8	41	12.7
Haiwee	Riverside	32.1	34.2	19	12.5
Haiwee	La Jolla	32.1	35.3	26	13.6
g) September 15, 1934, $06^h\ 56^m\ 59^s$, Mexico.					
Riverside	Haiwee	17.1	19.0	22	9.5
Pasadena	Tinemaha	17.7	19.9	25	9.8
Santa Barbara	Tinemaha	18.8	19.9	12	9.9
Pasadena	Haiwee	17.7	18.8	15	9.6
Tinemaha	Berkeley	19.9	22.7	27 ½	11.3
Santa Barbara	Berkeley	18.8	22.7	39 ½	10.9
Tinemaha	Stanford	19.9	22.3	26	10.4
Santa Barbara	Stanford	18.8	22.3	38	10.3
h) November 30, 1934, $02^h\ 05^m\ 19^s$, Mexico.					
La Jolla	Pasadena	17.1	18.6	18	9.1
Riverside	Haiwee	18.1	20.0	22	10.0
Pasadena	Tinemaha	18.6	20.9	26	10.1
Santa Barbara	Tinemaha	19.7	20.9	14	9.7
Pasadena	Haiwee	18.6	20.0	16	9.8
La Jolla	Santa Barbara	17.1	19.7	30	9.6
Tinemaha	Berkeley	20.9	23.6	27	10.9
Santa Barbara	Berkeley	19.7	23.6	41	10.5

In investigating Mexican shocks the authors[34]) found that a large increase in the amplitude of P occurs between $12^1/_2{}^\circ$ and 18° (see also figure 14). For the Atlantic shock of 1931 LEHMANN[39]) finds the ampli-

tudes still small at 15°, and noticeably larger at 17°—18°. The largest amplitudes were observed at about 20°. In the Iceland earthquake small amplitudes were observed at 12.2° and large amplitudes at 18.6°. For the Montana and Texas earthquakes amplitudes have been published by BYERLY[3, 4]). In the Montana shock Berkeley and Lick, distant 12°, recorded P with amplitudes of 11 μ and 2 μ; while at Pasadena (13.3°), the calculated amplitude is 55 μ. These seismograms are reproduced in BYERLY'S paper. For the Texas earthquake the calculated amplitude at six of the seven Southern California stations, at distances between $11^1/_2°$ and $13^1/_2°$ is less than one micron; but at La Jolla (about 11°) it is considerably larger. At Bozeman, Lick, Berkeley, and Chicago, with distances from 15.7° to 17.2°, the amplitude is well over one micron. At most of the remaining stations distant less than 27° the amplitudes were several microns.

All these data indicate that the amplitudes decrease rapidly from short distances up to about 14° (the exact value must vary with local structure, depth of focus, etc.) P is extremely small at about 12°—14°. At the end of this range there is a sudden increase, which seems to be followed by a gradual rise to a maximum about 20°, where the amplitudes are about as large as at 5°. Beyond 20° there is a slow falling off in amplitude. It is noteworthy that there is a sudden increase in the amplitude of PP at 27°, corresponding to P at $13^1/_2°$ (Sect. VII A).

We can now interpret these results in the light of the theoretical discussion in Section V. The nearly constant apparent velocity and small amplitudes observed between 6° and 14° are mutually consistent, and strongly indicate the conditions of case (18) of that Section. It follows that, in the range of depths reached by rays emerging at these distances, there can be no considerable increase of velocity with depth. The velocity may be closely constant, or may even decrease with depth. If it does not decrease with depth more rapidly than the very small limiting rate given by $dv/dr = v/r$, there are no special consequences of importance. However, it is physically possible that the velocity may decrease with depth at a rate somewhat in excess of this limit. If this actually occurs, the range from 6° to 14°, with its small amplitudes, corresponds to a so-called shadow zone, while the large amplitudes just beyond 14° may represent a focal point. It is not necessary to assume these conditions in order to explain the observations; indeed, the explanation does not appear to have a high degree of probability, as the apparent focus is hardly strong enough. In any case, the velocity

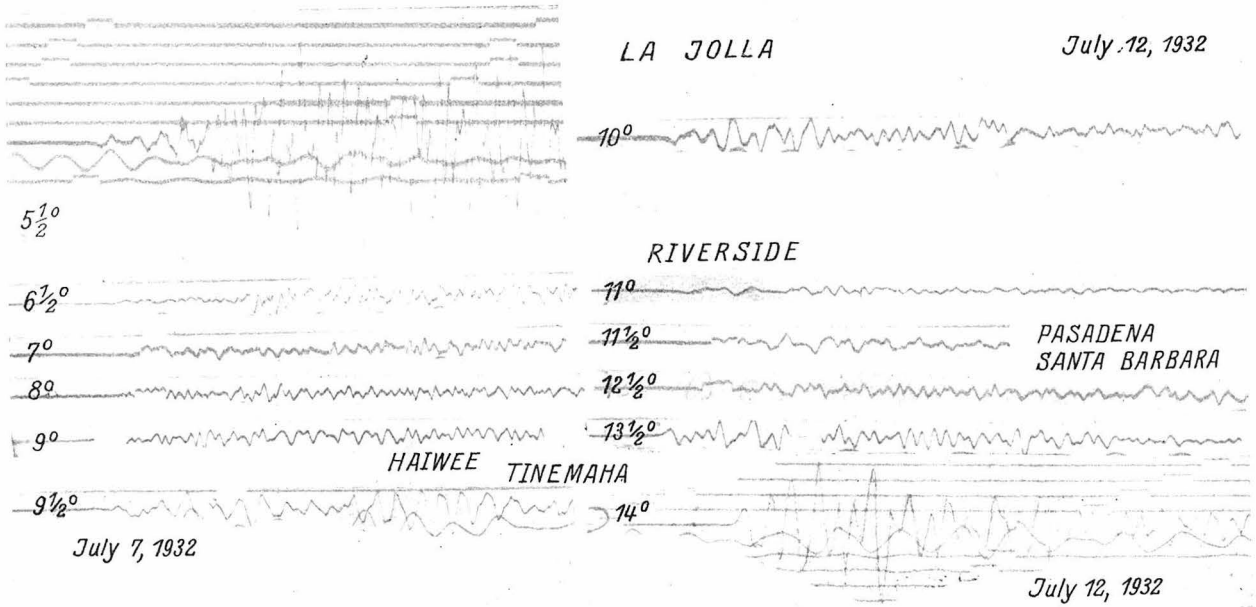

Fig. 14. Seismograms at short distances (5½°—14°). Shocks No. 110 and No. 111, Gulf of California.

cannot decrease very rapidly with depth, as otherwise the second branch of the travel time curve would fall too late after the projected course of the travel time curve for the diffracted waves; the observations show that the time interval cannot exceed a very few seconds.

Whatever the interpretation, the large amplitudes beyond 14° plainly imply a strong curvature of the travel time curve, and exclude any possibility of representing it as a series of nearly straight lines.

For these reasons, in calculating the distribution of velocity in depth, we shall assume that this distribution is continuous, and that the corresponding travel time curve is continuous, in the range of depth and distances which we have just been considering. No large errors can be introduced in this way.

While P is definite even when small, S usually cannot be identified unless it is rather large. The travel times consequently are well established only where large amplitudes occur. Further, the occurrence of large and small amplitudes cannot be used to draw conclusions as to the travel time curve, such as have been drawn for P, because of complications due to the polarization.

At short distances, especially under 15°, there are rapid changes with distance, both in the amplitude and in the time of S; there often is good evidence of multiplicity. Nevertheless, seismograms written at the same epicentral distance often show very close agreement, even at different stations and for different shocks (see Fig. 15). On the other hand, especially at the very shortest distances (under 10°) there are differences which may be attributed to differences in crustal structure or causative mechanism.

Up to about 6° the seismograms are of the local shock type; the S group of waves is usually conspicuous, and in many cases begins sharply with a phase having apparent velocity of 4.4 to 4.5 km./sec., which is identified as S_n. For the Southern California area this has been found to have travel times given by

$$S_n = 10.6 + \frac{\Delta\,(\text{km.})}{4.45}. \tag{22}$$

From 6° to 12° it usually is almost impossible to identify any S at all; there is continuous small, short-period motion which is finally superposed on a large long-period beginning of surface waves. At Pasadena, this is especially characteristic of the records of the nearer Mexican shocks. A very similar seismogram is that written at Kodiak, Alaska (distant 8.2°) on October 24, 1927, which has been published by

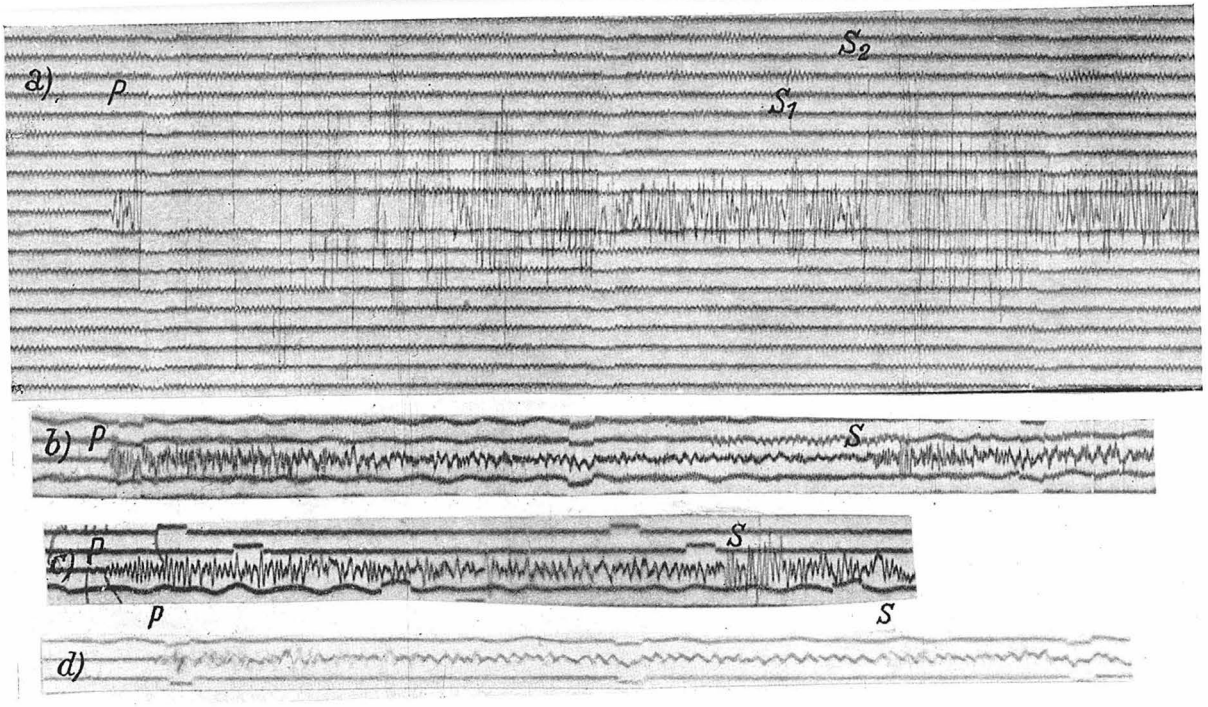

Fig. 15. Seismograms at distances of 8°—9°, showing short period S phases. (a), (c), (d), off Eureka, June 6, 1932; (b) Pacific Ocean southwest of Pasadena, Jan. 4, 1933. Instruments: (a) short-period BENIOFF NS; (b) ditto EW; both at Pasadena; (c) torsion EW, Santa Barbara; (d) torsion NS, Pasadena. The S wave is somewhat blurred in the reproduction.

H. H. Sommer[2]). The Texas and Utah shocks as recorded at Pasadena do not show the long periods so strongly; their place is taken by surface waves of shorter period, but also in these cases there is no clear indication of an S group.

The seismograms written at Pasadena for shocks in the region of Eureka, in northern California, at distances from $8^1/_2°$ to 9°, are exceptional. These records show a conspicuous short-period S, usually consisting of two sharp phases about ten seconds apart, the later having the larger amplitude. The earlier phase lies within the limits of error on the continuation of the S_n curve for local shocks in the region, as given by (22). Similar records are also written by shocks at about the same distance southwest of Pasadena, near 28° N. 126° W. Seismograms of both groups are shown in Fig. 15. Whatever the interpretation, this phenomenon is restricted to a very short range of distances; in the Eureka shocks it is well recorded at Pasadena and Santa Barbara, but is very doubtful at the other Southern California stations. That it is not restricted to this particular region is shown by the seismograms at Victoria for the Montana shock of 1925, which have been published by Byerly[4]). The distance is 8.4°, which is precisely that at which the effect is largest; and the seismograms plainly show the large sharp S. It is of interest to note that the record written at Göttingen for the Tuscan earthquake of Sept. 7, 1920, also shows something of the sort [22]). In this case the distance is considerably less (7.3°); but the large sharp S appears, and the record is not of the local-shock type.

Beyond 12° there are also occasional observations of points on the continuation of the local S_n curve (22), which in some cases are quite strong. An excellent instance is that of the Texas earthquake of 1931 as recorded at St. Louis and Florissant, distant 13.8°. These seismograms have been published by Byerly[3]). For the same shock, no corresponding phase can be found on the seismograms of stations at somewhat greater or smaller distances — Pasadena (12.3°), Tacubaya (12.3°), Haiwee (12.6°), Bozeman (15.7°), Lick (15.8°), Santa Clara (16.0°), Berkeley (16.4°).

From 12° onward there are numerous observations, mostly of eS, which plainly define a later curve than (22); this is for practical purposes the earliest definite S curve in the whole range from 12° to 60°. It corresponds to No. 2 of our first paper. As a larger body of observations can now be used, we give the following revised and extended travel times for this No. 2 S (minutes: seconds).

Dist. degr.	t No. 2	Dist. degr.	t No. 2	Dist. degr.	t No. 2
12	5:24	17	7:14	22	8:53
13	5:46	18	7:34	23	9:12
14	6:09	19	7:54	24	9:31
15	6:31	20	8:15	25	9:49
16	6:52	21	8:34	26	10:07

There are also many observations of iS following this eS; the phenomenon of eS preceding iS has been called the "curtsey" by BYERLY[3]). The readings of iS also define a curve, which coincides with No. 4 of the previous paper at the shorter distances, and appears then to pass into No. 5. Revised readings are as follows; the times are given in minutes and seconds.

Dist. degr.	t No. 4—5	Dist. degr.	t No. 4—5	Dist. degr.	t No. 4—5
16	7:10	21	8:47	26	10:16
17	7:28	22	9:06	27	10:34
18	7:47	23	9:25	28	10:52
19	8:07	24	9:43	29	11:09
20	8:28	25	10:01	30	11:24

Beginning at about 16° the amplitudes of this iS become very large, and remain so for a considerable range of distances. From about 20° on eS often appears as a large wave of long period.

From 12° to about 60° the No. 2 S very probably represents the true S curve corresponding to the first P. The conspicuous late iS at about 9°, discussed above, falls approximately on the extrapolation of the No. 2 S curve to short distances.

The occurrence of a double S phase at the short distances might be explained as due to a shadow zone with consequent diffraction; but the large amplitude at St. Louis for the Texas shock of 1931 makes this explanation questionable.

XI. Calculation for velocities of P and S at various depths in the mantle.

Calculated velocities for P in the mantle have been based on the travel times for P given in Table 5 of the first paper and on the data for apparent velocities at the shorter distances given in the present paper (table 15 and fig. 13). It is necessary to make some assumption as to the end of the direct P curve, beyond which only diffracted P

waves are recorded. This point has been taken at $\Delta = 11500$ km. ($103^1/_2°$), since the amplitudes decrease very rapidly beyond that distance.

The effect of the crustal layers has been eliminated by reducing the observed travel times to those at a depth of 40 km., which is taken as the base of the crust. The mean velocity in the crustal layer is assumed to be about 6 km./sec., and the depth of focus to be 25 km. This gives the following approximate corrections to the travel time curve:

$$(23)\quad \delta\Delta = (2\,d - h)\tan i = 55 \tan i \text{ km.} \qquad \delta t = \frac{2\,d - h}{V \cos i} = \frac{9 \sec}{\cos i}.$$

The error in applying these formulae is very slight, and they have been used exactly throughout the whole range. The values of $\delta\Delta$ are all less than $½°$, and those of δt decrease from 12 to 9 seconds, in passing from 15° to the end of the curve. The procedure gives a travel time curve for a depth of 40 km. From this reduced curve we have calculated the apparent velocities, taken their reciprocals, and used the formula $t = \int \frac{d\Delta}{v}$ to adjust them to the assumed curve. In this adjustment we have taken account of the observed amplitudes; pains have been taken to make those parts of the curve where the apparent velocity is nearly constant correspond to small observed amplitudes, and those parts where the apparent velocity changes rapidly with distance correspond to large amplitudes. In some cases this has required changing the travel times by one second.

The results of this process of adjustment are fundamental to the following calculations, and are therefore given in Tables 16 and 17.

The well-known method of WIECHERT, HERGLOTZ, and BATEMAN has been applied to the data of Tables 16 and 17. The results are given in Table 18. In this table the first column gives the distance in megameters, measured at the level 40 km. below the surface, at which the ray which has touched the level given by the depth d at its deepest point emerges to the 40 km. level. The final value in the table corresponds to the ray which has grazed the core, which accordingly is thus placed at a depth of 2920 km. The corresponding value of v, v_c, can be computed by an independent method; for it must satisfy the relation

$$(24)\qquad v_c = \frac{r_c}{r_0}\,\bar{v}_d\,,$$

where r_c is the radius of the core, r_0 that of the earth, and $\bar{v}_d$ is the apparent velocity of the diffracted P waves at the surface of the earth.

Table 16.

Apparent velocities $\bar{v}$ of P-waves and reciprocals $1/\bar{v}$ for distances Δ in units of 1000 km. (megameters) for arrival at a depth of 40 km.

Δ	$\bar{v}$	$1/\bar{v}$	Δ	$\bar{v}$	$1/\bar{v}$	Δ	$\bar{v}$	$1/\bar{v}$
0.0	7.85	.127	4.8	13.33	.0750	8.2	19.61	.0510
1.4	7.85	127	5.0	13.77	0726	8.4	20.28	0493
1.6	8.26	121	5.2	14.31	0699	8.6	20.41	0490
1.8	9.43	106	5.4	14.79	0676	8.8	20.62	0485
2.0	9.90	101	5.6	15.08	0663	9.0	21.28	0470
2.2	10.36	0965	5.8	15.27	0665	9.2	21.98	0455
2.4	10.83	0923	6.0	15.46	0647	9.4	22.22	0450
2.6	11.30	0885	6.2	15.58	0642	9.6	22.27	0449
2.8	11.72	0853	6.4	15.75	0635	9.8	22.57	0443
3.0	12.11	0826	6.6	15.90	0629	10.0	23.09	0433
3.2	12.48	0801	6.8	16.05	0623	10.2	23.87	0419
3.4	12.79	0782	7.0	16.26	0615	10.4	24.75	0404
3.6	12.95	0772	7.2	16.53	0605	10.6	25.00	0400
3.8	13.11	0763	7.4	17.01	0588	10.8	25.06	0399
4.0	13.19	0758	7.5	17.39	0575	11.0	25.12	0398
4.2	13.23	0756	7.6	17.45	0573	11.2	25.19	0397
4.4	13.25	0755	7.8	18.08	0553	11.4	25.23	0396
4.6	13.25	0755	8.0	18.87	0530	11.5	25.25	0396

Table 17.

Travel times t in seconds for arrival of P-waves at a depth of 40 km. corresponding to the apparent velocities given in table 16.

Δ	t	Δ	t	Δ	t
1.2	153	4.6	462	7.7	663
1.5	191	4.8	477	8.0	679
1.8	225	5.0	491	8.4	699
2.0	246	5.2	505	8.7	715
2.3	276	5.4	518	9.0	729
2.5	294	5.6	531	9.2	738
2.7	312	5.8	545	9.5	752
3.0	337	6.0	557	10.0	774
3.3	361	6.3	578	10.1	778
3.5	377	6.5	590	10.3	785
3.8	400	6.8	610	10.5	793
4.0	415	7.0	622	10.7	802
4.2	431	7.2	634	11.0	813
4.4	447	7.5	652	11.5	833

Table 18.
Velocity v of P in the mantle as a function of depth $d = r_0 - r_s$ and corresponding distances Δ at the 40 km. level.

Δ	d km.	v km./sec.	Δ	d km.	v km./sec.	Δ	d km.	v km./sec.
1.6	200	8.1	5.2	1180	11.7	8.4	2250	13.2
1.8	360	9.0	5.6	1330	12.0	8.8	2340	13.2
2.4	550	10.2	6.0	1400	12.1	9.2	2490	13.5
3.0	720	10.8	6.6	1500	12.2	9.8	2580	13.5
3.6	860	11.3	7.2	1610	12.4	10.4	2850	13.8
4.0	920	11.4	7.5	1810	12.5	11.5	2920	13.7
4.8	960	11.4	7.6	1820	12.5			
5.0	1070	11.5	8.0	2050	12.9			

The apparent velocity used for this purpose has been taken from the data of Table 5 of the first paper. Only points from 105° to 132° have been used, as for larger distances the observations probably refer to later phases. The value which best represents the observations in this range is $\bar{v}_d = 25.2$ km./sec. The corresponding value of v_c is found to be 13.7 km./sec., which agrees precisely with that given in the table.

The data of Table 18 are represented graphically in Fig. 16. Within the mantle the curve is in general smooth; irregularities appear at depths of about 1000 km., 1800 km., and 2300 km. The first of these is less well marked, and at less depth, than was concluded in the earliest investigations. This is actually the same discontinuity which was first discussed by WIECHERT; the corresponding rays emerge at about the same distance as found by him. The decreased depth is due to the general improvement in observed travel times. The determination of this depth involves the observations up to about 45°.

The existence of such discontinuities within the mantle would imply a possibility of observing waves reflected at the levels in question. In the first paper it was pointed out that certain observations lie on curves (designated as A, B, and E) which have the characteristic form to be expected for such reflections. Accordingly, times have been calculated for reflections at depths of 930, 1800, and 2250 km. The first two cases correspond to no identifiable observations. For 2250 km. we find times for the reflected longitudinal wave of $7^m\ 45^s$ at 26.2°, $8^m\ 10^s$ at 33.2°, and $8^m\ 31^s$ at 36.6°. These values are about half a minute less than the observed times for phase A. Consequently, if A is a reflect-

ed wave, the reflecting layer lies about 200 km. deeper than has been assumed; it is not impossible that a discontinuity exists at about 2400 km. (See Fig. 16.) *B* should be reflected at still greater depth. The corresponding travel times for transverse waves have been computed, using the data which will be given below. For reflection at 2250 km. we find 14.0^m at 27.7°, 14.9^m at 34.8°, and 15.4^m at 39.1°. These values are about 0.8^m earlier than those observed for *E*, which would indicate a reflecting surface at about the same depth as found for *A*.

Similar computations have of course been made for reflection at the depth of 2920 km., assumed to be that of the core. These should give the travel times of *PcP*, and comparison with observations accordingly affords a check on the assumed depth. As always, a focal depth of 25 km. has been assumed; the calculations give the following results:

Distance degrees	*t PcP* min.:sec.	Distance degrees	*t PcP* min.:sec.	Distance degrees	min.:sec. *t PcP*
0.0	8:38	35.2	9:29	68.0	11:25
13.9	8:40	41.9	9:51	78.6	12:10
21.0	8:52	48.0	10:11		
28.1	9:11	56.5	10:41		

Between 30° and 50° these calculated times are about ten seconds earlier than those found from observations in our first paper. Between 50° and 65° they agree with the observations within one second. For the range between 20° and 80° the calculations agree within two seconds with the observed travel times used by DAHM[40]). In general, observations and calculations thus agree well within the limits of error; it appears safe to conclude that there is no considerable error in the velocity distribution of Table 18, or in the depth of the core.

In spite of this good agreement, it must not be assumed that the depth of the core is determined as precisely 2920 km. This figure may easily be in error by as much as 50 km. The following seem to be the principal sources of uncertainty: (a) the mean velocity in the crustal layers, which we have taken as 6 km./sec., but which may differ from this and may vary in different regions; (b) the thickness of the crust, which certainly varies from point to point; (c) the depth of focus, which undoubtedly varies considerably even for shocks of "normal" focal depth; (d) the inaccuracy of the observed travel times of *P*, especially beyond 100°; (e) inaccuracy in the determination of the

point at which the "shadow zone" begins. The combined effect of errors in (a), (b), and (c) can hardly exceed four seconds in the travel times. (d) is more serious, as the beginning of P in the critical range is never large or sharp, and the possibility of multiplicity still further complicates the interpretation. (e) is fortunately not a large source of error; for although it is difficult to determine the point at which the

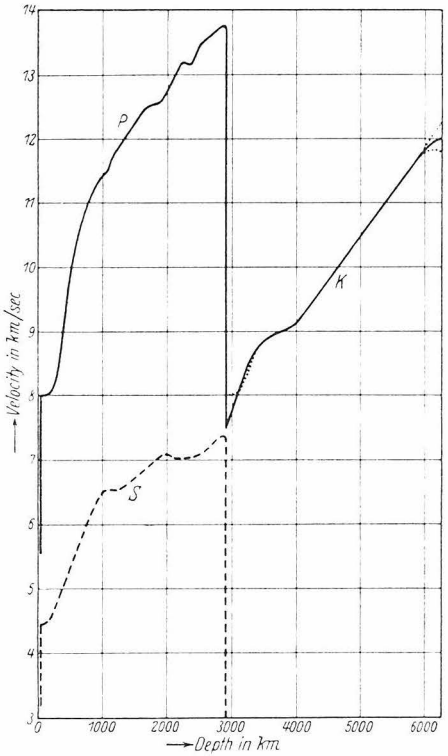

Fig. 16.
Velocities of seismic waves in the interior of the earth, as functions of depth.

shadow zone begins, the effect of uncertainty on the calculated depth of the core is not likely to exceed 30 km.

DAHM[40]) has recently arrived at conclusions with regard to the velocity in the deeper part of the mantle which differ from those of previous investigators as well as those of the present paper. He finds that the velocity increases to 13.45 km./sec. at a depth of 2780 km., where there is a discontinuity. Below this depth he finds a constant velocity of 12.57 km./sec. to the surface of the core, which he places at about 3000 km. This interpretation by DAHM depends on the circumstances mentioned under (d). He has used observations which give

apparent velocities beyond 100° only slightly different from those found from the data of our first paper. Calculations using these data then give the maximum velocity at 2780 km., and in order to account for the observed *PcP* it is then necessary to assume a discontinuity, with the core at greater depth. This is a good example of the very considerable differences in results which may be obtained with slight changes in the data.

It is desirable to apply the same general procedure to the observations of *S*. Unfortunately, the data are not so good as for *P*, and the results cannot be received with as much confidence. Before commencing computation it is of course necessary to adopt a representative travel time curve for *S*. The discussion in section X of the present paper will serve to bring out the difficulty of doing this. For the shortest distances we have used the travel time of S_n in local shocks; from 16° to about 60° we have tried to use the No. 2 curve of our first paper, with revised readings as given in Section X of the present paper. However, it has proved impossible to carry out the suggestion in the first paper that the No. 2 curve is separately continuous through 65°. In order to avoid peculiar results as to the velocity distribution with depth, it was necessary to connect the No. 2 curve below 66° with the No. 1 curve above it, making the transition as gradual as possible. This does no violence to the observations, which are rather uncertain, as the amplitude of *S* is often small in this range.

The adopted values of the travel times for *S* are given in Table 19. These were subjected to the same adjustments and reductions as the

Table 19.

Adopted travel times of *S*. (Distances θ in degrees, times t in minutes : seconds.)

θ	t	θ	t	θ	t	θ	t	θ	t
2	1:00	22	8:54	42	14:10	62	18:44	82	22:30
4	1:51	24	9:31	44	14:39	64	19:08	84	22:52
6	2:42	26	10:07	46	15:08	66	19:31	86	23:14
8	3:32	28	10:40	48	15:36	68	19:54	88	23:35
10	4:23	30	11:11	50	16:03	70	20:17	90	23:54
12	5:13	32	11:42	52	16:31	72	20:39	92	24:11
14	6:04	34	12:12	54	17:00	74	21:01	94	24:28
16	6:52	36	12:42	56	17:28	76	21:23	96	24:45
18	7:35	38	13:13	58	17:55	78	21:45	98	25:01
20	8:16	40	13:43	60	18:20	80	22:07	100	25:18

Table 20.

Apparent velocities $\bar{v}$ of S-waves and reciprocals $1/\bar{v}$ for distances Δ in megameters for arrival at a depth of 40 km.

Δ	$\bar{v}$	$1/\bar{v}$	Δ	$\bar{v}$	$1/\bar{v}$	Δ	$\bar{v}$	$1/\bar{v}$
0.0	4.40	.228	4.2	7.69	.130	8.0	10.10	.099
1.5	4.41	.227	4.4	7.75	.129	8.2	10.20	.098
1.6	4.57	.219	4.6	7.81	.128	8.8	10.20	.098
1.8	4.93	.203	4.8	7.81	.128	9.0	10.31	.097
2.0	5.29	.189	5.0	7.87	.127	9.4	10.31	.097
2.2	5.62	.178	6.0	7.87	.127	9.6	10.42	.096
2.4	5.95	.168	6.2	8.06	.124	9.8	10.53	.095
2.6	6.25	.160	6.4	8.33	.120	10.0	10.99	.091
2.8	6.54	.153	6.6	8.77	.114	10.2	11.63	.086
3.0	6.80	.147	6.8	9.09	.110	10.4	12.50	.080
3.2	6.99	.143	7.0	9.35	.107	10.6	13.15	.076
3.4	7.19	.139	7.2	9.52	.105	10.8	13.30	.075
3.6	7.30	.137	7.4	9.71	.103	11.0	13.30	.075
3.8	7.46	.134	7.6	9.90	.101	11.2	13.30	.075
4.0	7.58	.132	7.8	10.00	.100	11.4	13.30	.075

travel times for P; Tables 20, 21 and 22 give the data corresponding to those given for P in Tables 16, 17 and 18.

The velocities (Table 22) have been plotted in Fig. 16. The fact that the indicated discontinuities do not agree precisely with those found from P is to be accounted for by the difficulties of reading and interpretation for S, though some real differences may exist.

In applying this procedure, the observed amplitudes could not be used in the same way as was done for P. It has been assumed that the shadow zone for S begins at 10800 km., as for larger distances the apparent velocity is constant, about 13.3 km./sec. Supposing that the

Table 21.

Travel times t in seconds for arrival of S-waves at a depth of 40 km. corresponding to the apparent velocities given in table 20.

Δ	t	Δ	t	Δ	t
1.5	341	5.0	877	8.5	1273
2.0	445	5.5	940	9.0	1322
2.5	533	6.0	1004	9.5	1370
3.0	610	6.5	1066	10.0	1417
3.5	681	7.0	1121	10.5	1459
4.0	748	7.5	1174	11.0	1496
4.5	813	8.0	1223		

Table 22.
Velocity v of S in the mantle as a function of the depth $d = r_0 - r_s$ and corresponding distances Δ at the 40 km. level.

Δ	d km.	v km./sec.	Δ	d km.	v km./sec.	Δ	d km.	v km./sec.
1.6	180	4.5	5.0	1090	6.6	9.6	2100	7.0
2.0	380	5.0	6.2	1220	6.6	9.8	2150	7.0
2.4	550	5.5	6.6	1510	6.7	10.0	2320	7.0
2.8	690	5.9	7.0	1700	6.9	10.4	2720	7.2
3.2	800	6.2	7.4	1820	7.0	10.8	2960	7.3
3.8	930	6.4	7.8	1910	7.1			
4.4	1030	6.5	8.2	1980	7.1			

correct depth of the core is 2920 km., as found from P, equation (24) gives a velocity of 7.2 km./sec. for transverse waves at the outer surface of the core. This corresponds very well with the result given in Table 22.

The travel times of *ScS* have been calculated in the same way as those for *PcP*. The results are as follows:

Distance degrees	*t ScS* min.:sec.	Distance degrees	*t ScS* min.:sec.	Distance degrees	*t ScS* min.:sec.
0.0	15:38	36.1	17:22	69.4	21:13
14.3	15:55	43.0	18:02	80.5	22:32
21.5	16:15	49.3	18:40		
28.8	16:41	58.7	19:41		

These calculations agree within a few seconds with the observed travel times for the No. 1 *ScS* curve given in the first paper. Beyond 50° the observations are later; but these observations had already been recognized as belonging to later phases (Nos. 2, 3, 4).

Representative times have been calculated for *PcS*, as follows:

Distance	22½	34	44	66 degrees
t PcS.	12.4	13.0	13.7	15.4 minutes

Theoretically the curve ends at about 66°. The *PcS* curve given in Fig. 11 of the first paper agrees with these calculations within the limits of error.

XII. Velocity distribution within the core.

In previous investigations the velocity within the core has been found from the observed travel times of P' by a process of trial and error. A recent suggestion by Wadati and Masuda[41]) provides a new and valuable method which leads directly to the travel times between

points at the surface of the core; the usual method of integration can then be applied to these data, and the velocity distribution within the core calculated at once.

WADATI and MASUDA propose to derive travel times through the core by subtracting each observed arrival time of *ScS* at the surface of the earth from the arrival time of the corresponding *SKS* wave which has the same angle of emergence at the surface. The procedure is to find $dt/d\theta$ for both curves, and to take the differences of times which correspond to equal values of $dt/d\theta$, and the corresponding differences in the angular distances, θ. This gives the travel time through the core as a function of θ. The advantage of using *SKS* and *ScS* is that it becomes possible to find travel times for small values of θ. Unfortunately, the method cannot at present be applied to very small values of θ, as the *SKS* curve is not well observed at distances less than that of its intersection with *S* (about 84° for normal shocks.)

Table 23.
Calculated travel times between points on the surface of the core.

Phases used a)	b)	$\bar{v}$ km./sec.	θ a) degr.	θ b) degr.	t a) min.:sec.	t b) min.:sec.	θ in core degr.	t in core min.:sec.
SKS	*ScS*	18½	79	40½	22:25?	17:40	38½	4:45?
		19	84	40½	22:51	17:40	43½	5:11
		20	96	37½	23:57	17:23	58½	6:43
		22	106	33	24:49	16:57	73	7:52
		25	114	28	25:28	16:32	86	8:56
		30	120	23½	25:51	16:14	96½	9:37
		46	130	14½	26:18?	15:48	115½	10:30?
		93	155	7	27:00?	15:34	148	11:26?
P_2'	*PcP*	25	180	106	22:15	14:13	74	8:02
P'	*PcP*	29	142	57	19:27	10:44	85	8:43
		55	148	24	19:45	8:58	124	10:47
		65	153	19	19:53	8:47	134	11:06
		100	157	12	19:58	8:37	145	11:21
		200	166	6	20:05	8:33	160	11:32
		∞	180	0	20:09	8:33	180	11:36
SKP	*PcS*	28	132	44	22:47	13:46	88	9:01
		32	136	34	22:54	13:07	102	9:47
		44	142	22½	23:15	12:30	119½	10:45
PKKP	*PcP*	40	263	34	30:24	9:26	114½	10:29
		37	257	38	30:06	9:37	109½	10:14
		32	247	47½	29:33	10:09	100	9:42
SKKS	*ScS*	18½?	74	40½	22:16	17:40	17?	2:18?

We have extended this method by applying it to other pairs of observed phases. (This has also been done by JEFFREYS; private communication.) None of these give good points for very small values of θ, but they supply additional points at various distances so that finally the curve is well determined for a large range. The results are presented in table 23.

The relation of P' or P_2' to PcP, or of SKP to ScP, is plainly the same as that of SKS to ScS. Subtracting corresponding times and distances in the case of $PKKP$ and PcP, or of $SKKS$ and ScS, yields double the times and distances for the core. There are other possible com-

Table 24.

Adopted travel times t between points on the surface of the core, and reciprocals $1/v$ of the apparent velocity.

θ degr.	t min.:sec.	$1/v$ sec./km.	θ degr.	t min.:sec.	$1/v$ sec./km.	θ degr.	t min.:sec.	$1/v$ sec./km.
2	0:16	0.133	56	6:23	0.095	110	10:16	0.044
4	0:32	133	58	6:34	93	112	10:21	43
6	0:48	133	60	6:45	92	114	10:26	41
8	1:04	132	62	6:56	91	116	10:31	40
10	1:19	130	64	7:07	90	118	10:36	39
12	1:35	129	66	7:18	89	120	10:40	38
14	1:50	128	68	7:29	88	122	10:45	37
16	2:05	127	70	7:39	86	124	10:49	36
18	2:20	125	72	7:49	84	126	10:53	35
20	2:35	122	74	7:59	83	128	10:57	33
22	2:49	120	76	8:09	82	130	11:01	30
24	3:04	117	78	8:19	81	132	11:04	27
26	3:18	116	80	8:28	79	134	11:07	25
28	3:32	115	82	8:37	76	136	11:09	23
30	3:45	113	84	8:46	73	138	11:12	21
32	3:58	111	86	8:54	70	140	11:15	19
34	4:11	108	88	9:03	68	142	11:17	18
36	4:24	106	90	9:11	66	144	11:19	17
38	4:37	104	92	9:18	64	146	11:21	16
40	4:49	102	94	9:26	62	148	11:23	15
42	5:01	100	96	9:33	60	150	11:25	15
44	5:13	100	98	9:40	58	152	11:26	14
46	5:25	098	100	9:47	56	154	11:28	14
48	5:37	098	102	9:53	53	156	11:29	13
50	5:49	097	104	9:59	51	158	11:31	12
52	6:00	097	106	10:05	49	160	11:32	12
54	6:12	096	108	10:11	46	180	11:36	00

binations, but these do not yield accurate results. It should be observed that the results from different combinations in Table 23 agree very well with each other; the entire set of points defines a very smooth curve, which is given in tabular form as Table 24. Unfortunately, no points are available to define the curve for the shortest distances; but the range of reasonable possibilities is rather limited. Using the values of $1/v$ in the same table, the velocity as a function of depth has been calculated, and is given in Table 25. The same results are plotted in Figure 16. The beginning and end of the curve are uncertain by about half a kilometer per second; this is indicated by the dotted lines in the figure. Allowing for this, the whole curve for the core can be represented closely by the linear relation $v = 12.13 - 0.00121\ r$. On the other hand, the travel time curve very clearly indicates that such a

Table 25.

Velocity v of waves in the core as a function of r_s and of $d = r_0 - r_s$, and corresponding angular distances θ at the surface of the core.

θ degrees	r_s km.	d km.	v km./sec.
0	3446	2920	7½—8
30	3200	3170	8.3
41	3010	3350	8.7
60	2810	3550	8.9
75	2550	3820	9.0
90	2130	4240	9.5
105	1680	4690	10.0
120	1350	5010	10.5
150	580	5800	11.5
180	0	6370	12

linear variation with depth cannot be exact, as the observational divergences are outside the limits of error. Moreover, for physical reasons, one would expect the correct curve for Fig. 16 to have a horizontal tangent for the center of the earth. The observations give no light on this, as even the uncertainty indicated by the dotted line in the figure corresponds to differences in the travel times of less than one second.

It is very satisfactory that the velocity distribution found by this new method agrees very well with those found in previous investigations. The agreement is especially close with the recent results of WADATI and MASUDA[41]), who have used differences of *SKS* and *ScS* to fix certain points.

From the result already given the travel times for P', P_2', PKS, SKS, and $PKKP$, have been calculated. These are given in Table 26. In general these times agree very closely with the observations, except in the neighborhood of the focal points. The distance of the focal point in each case is correctly given by the minimum of the travel time; but this calculated time is later than that observed at the focal point by about 10 seconds for P', 7 seconds for PKS, and 20 seconds for $PKKP$. It is noteworthy that this discrepancy for $PKKP$ is about double that for P'. It is too large to be accounted for by any reasonable change in the velocity distribution. For SKS, which has no focus, the observations are everywhere within five seconds of the calculated times. The effect is presumably connected with the large concentration of energy near the focal points, which may result in earlier observations.

For $PKKS$ the observations are not good enough for comparison with the calculated times, which serve only to establish that this phase is recorded.

The observations of $SKKS$ are about $^1/_4$ minute earlier than the calculated values, where this comparison is possible.

Table 26.

Calculated arrival times for core waves at the surface of the earth.

Distance degrees	$t\ P'$ min.:sec.	Distance degrees	$t\ SKP$ min.:sec.	Distance degrees	$t\ PKKS$ min.:sec.
160½	20:44	136	23:00	138	31:54
151	20:07	133	22:47	134	32:12
147	19:54	132	22:45	130	32:28
141½	19:36	133	22:50	126	32:38
146	19:44	134	22:51	121	32:55
151	19:51	136	22:55		
166	20:06				
	$t\ SKS$		$t\ PKKP$		$t\ SKKS$
84	22:48	73½	29:38	124	27:37
91	23:33	119	29:17	141	29:22
98	24:11	116	29:33	158	30:57
103½	24:43	112½	29:40	173½	32:23
110½	25:11	103½	30:06	169½	33:39
115	25:30	96	30:21	161½	34:13
119½	25:49	89	30:34	155	34:40
123½	26:02			149	35:07
126	26:08				
129	26:15				

XIII. Calculated and observed travel times; additional data.

Comparison of observations of *PP*, *P'P'*, and *SS* with times calculated from the observations of *P*, *P'*, and *S* will be found in the first paper (section X, p. 95; section XII, p. 97; section XV, p. 107).

In the present paper we have already compared the times calculated from the velocity distribution with those observed for *P*, *S*, *PcP*, *ScS*, *PcS* (section XI) and for *P'*, *SKP*, *SKS*, *PKKP*, *SKKS* (section XII).

Travel times for *PS* and *PPS* cannot be calculated with any great precision, as the result depends on a correspondence between the apparent surface velocities of *P* and *S*, both of which change very slowly at certain distances. Theoretically *PS* and *PPS* branch from *S* at about 50°.

Observations of *PS* begin at about 70° (Table 14, first paper; there are a few doubtful observations at shorter distances), with times 12 to 14 seconds later than those calculated. Observations then approach the calculated times, and agree fairly well about 110° to 115°. At larger distances the observed *PS* (No. 2) is again late — about 20 sec. at 120° and about 30 sec. at 130°.

Comparison of observed with calculated *PPS* is still more uncertain, because of multiplicity in both *PS* and *PPS*, the possibility of *PPPS*, etc. At distances under 100° the observations agree with the calculated times to within 0.3 minute; at large distances the observed values are up to half a minute late. It should be noticed that the times given in the first paper for these large distances are not the earliest observed, but simply the mean values of scattered points.

SKSP is well observed beyond 130°. The values calculated from the velocities agree with these observations within $^1/_4$ minute.

SKPP' is well observed only in deep-focus shocks. For normal shocks we calculate a focus at about 86°, with a time of 42.4^m.

In section XXVI of the first paper we have discussed the group of more complicated waves reflected from the outer surface of the core, and have made some comparisons with observation. The most important waves of this type are *ScSP*, *ScSP'*, *PcPP'*, and *ScSScS*.

It was mentioned in the first paper (p. 122) that calculation for *ScSP* is very uncertain, the results being extremely sensitive to small changes in the data. With the new velocities we find a focal point at 113°, 29^m 16^s; this replaces the values 77°, 25^m, given in the first paper. This agrees very well with the values 111°, 28^m 57^s, given by JEFFREYS

in mimeographed seismic transmission times recently (1935) issued in extension of the work of JEFFREYS and BULLEN[44]). We are indebted to Dr. JEFFREYS for calling our attention to the circumstance. It follows that the observations attributed to *ScSP* in the first paper refer either to diffracted waves, or to late members of the *PS* group.

The focal point of *ScSP'* is of interest, as it falls in the range of distances and times where *S'* has been suspected. We now find it at $158^1/_2°$, $35^m\ 28^s$. JEFFREYS (1935) gives 159°, $35^m\ 26.5^s$.

The corresponding point for *PcPP'* is now found at 169°, $28^m\ 35^s$. The times for *ScSScS* are easily calculated from those for *ScS*. In the range of best observations, about 100°, the calculated times agree within a few seconds.

There are no further phases which are at present well enough observed to check against calculations; and as the agreement in all available cases is now within the limits of observational error, it is not likely that any considerable changes in the travel time tabulations or in the velocities will be necessary in the future.

XIV. Poisson's Ratio.

It is of some interest to calculate POISSON's ratio σ for various depths in the mantle. σ is given by the formula

$$\sigma = \frac{1}{2} - \frac{1}{2\left[\left(\frac{V}{v}\right)^2 - 1\right]}, \tag{25}$$

where V is the velocity of longitudinal waves, and v that of transverse waves. Using the velocities given in tables 18 and 22, the results are as follows:

Table 27.

POISSON's Ratio σ as function of depth.

Depth . . .	50	500	1000	1500	2000	2500	2900	km.
σ	.28	.29	.26	.28	.28	.30	.30	

References.

1. B. GUTENBERG and C. F. RICHTER, On seismic waves (first paper). Gerl. Beitr. Geophys. **43** (1934) 56. — 2. H. H. SOMMER, On the question of dispersion in the first preliminary seismic waves. Bull. Seism. Soc. Amer. **21** (1931) 87. — 3. P. BYERLY, The Texas Earthquake of August 16, 1931. Bull. Seism. Soc. Amer. **24** (1934) 81. — 4. P. BYERLY, The Montana Earthquake of June 28, 1925. Bull. Seism. Soc. Amer. **16** (1926) 209. — 5. B. GUTENBERG, Periods of the ground in Southern California Earthquakes. In press, U. S. Coast and Geodetic Survey, Washington D. C. — 6. S. NAKAMURA, Journ.

Meteorol. Soc. Japan **1** (Febr. 1922) 43, and **1** (March 1923) 69. — K. Suda, Memoirs Imp. Marine Obs. Kobe **1** (1924) No. 4. — A. Imamura, Preliminary note on the great earthquake of S.E. Japan on Sept. 1, 1923. Imp. Earthquake Invest. Comm., Seismol. Notes, No. 6. Tokyo 1924. — 7. E. Gherzi, Notes de sismologie, Observatoire de Zi-Ka-Wei, No. 4, 1923; No. 6, 1925; No. 10, 1929. — 8. O. Somville, Sur la nature de l'onde initiale des téléséismes enregistrés à Uccle de 1910 à 1924. Publ. du Bureau Centr. Seismolog. Int. (A) **2** (1925) 65. — 9. L. Geiger und B. Gutenberg, Über Erdbebenwellen. VI. Nachr. Ges. Wiss. Göttingen, math.-phys. Kl. **1912**, 623. — 10. H. Jeffreys, The reflection and refraction of elastic waves. Mthly Not. Roy. Astron. Soc., Geophys. Suppl. **1** (1926) 321. — 11. K. Zoeppritz, Über Erdbebenwellen. VII b. Nachr. Ges. Wiss. Göttingen, math.-phys. Kl. **1919**, 57. — 12. K. Zoeppritz, L. Geiger und B. Gutenberg, Über Erdbebenwellen. V. Nachr. Ges. Wiss. Göttingen, math.-phys. Kl. **1912**, 121. — 13. C. G. Knott, The propagation of earthquake waves through the earth. Proc. Edinburgh **28** (1918/19) 217. — 14. C. G. Knott, Reflexion and refraction of elastic waves, with seismological applications. Philos. Mag. **48** (1899) 64. — 15. L. B. Slichter and V. G. Gabriel, Studies in reflected seismic waves. Gerl. Beitr. Geophys. **38** (1933) 228. — 16. H. P. Berlage, Näherungsformeln zur Berechnung der Amplituden der elastischen Wellen. Gerl. Beitr. Geophys. **26** (1930) 131. — 17. H. Blut, Ein Beitrag zur Theorie der Reflexion und Brechung elastischer Wellen an Unstetigkeitsflächen. Z. Geophys. **8** (1932) 130 and 305. — 18. L. B. Slichter, The theory of the interpretation of seismic travel time curves in horizontal structures. Physics **3** (1932) 273. — 19. H. Witte, Beiträge zur Berechnung der Geschwindigkeit der Raumwellen im Erdinnern. Nachr. Ges. Wiss. Göttingen, math.-phys. Kl. **1932**, 199. — 20. H. Jung, Über Erdbebenwellen. IX. Nachr. Ges. Wiss. Göttingen, math.-phys. Kl. **1933**, 42. — 21. H. Kawasumi and R. Yosiyama, On the mechanism of a deep-seated earthquake ... Proc. Imp. Acad. Tokyo **10** (1934) 345. — 22. Mitteilungen der deutschen Erdbebenwarten, herausgegeben von der Hauptstation für Erdbebenforschung in Jena. 1921/22. Tafeln 9—19. — 23. E. Wanner, Beiträge zum Studium der *PS*-Phase und Mächtigkeit der Molasse unterhalb Zürich. Gerl. Beitr. Geophys. **32** (1931) 231. — 24. B. Galitzin, Über die Schwingungsrichtung eines Bodenteilchens in den transversalen Wellen der zweiten Vorphase eines Bebens. Bull. Acad. Imp. des Sciences de St. Pétersbourg **1911**, 1019. — 25. B. Gutenberg and C. F. Richter, On $P'P'$ and related waves. Gerl. Beitr. Geophys. **41** (1934) 149. — 26. J. Milne, Eighth report of the Comm. on Seismol. Investigations. Southport (1903). — 27. W. Láska, Über die Verwendung der Erdbebenbeobachtungen zur Erforschung des Erdinnern. Mitt. Erdbebenkomm. Wien. N. F. **23** (1904). — 28. H. Benndorf, Über die Art der Fortpflanzung der Erdbebenwellen im Erdinnern. Mitt. Erdbebenkomm. Wien. N. F. **29** (1905) and **31** (1906). — 29. S. Mohorovičić, Die reduzierte Laufzeitkurve und die Abhängigkeit der Herdtiefe ... II. Gerl. Beitr. Geophys. **14** (1916) 187. — 30. A. Mohorovičić, Hodograph der ersten longitudinalen Wellen eines Bebens. Acad. Zagreb, Bull. **2** (1914). — 31. B. Galitzin, Sur l'angle d'émergence des rayons sismiques. Nachr. der seism. Komm., Petersburg **7** (1917). —

32. J. Wilip, Emergenzwinkel, Unstetigkeitsflächen, Laufzeit. Acta et Commentationes Universitatis Dorpatensis. A. VI. 10. Dorpat 1924. — 33. B. Gutenberg, Untersuchungen zur Frage, bis zu welcher Tiefe die Erde kristallin ist. Z. Geophys. **2** (1926) 24. — 34. B. Gutenberg and C. F. Richter, On supposed discontinuities in the mantle of the earth. Bull. Seism. Soc. Amer. **21** (1931) 216. — 35. F. Neumann, The transmission of seismic waves. Trans. Amer. Geophys. Union, 14. annual meeting, Washington **1933**, 329. — 36. F. Neumann, A further note on the interpretation of travel time curves. (Abstract.) Earthquake Notes. Washington **6** (1934) 20. — 37. P. Byerly, The first preliminary waves of the Nevada Earthquake of December 20, 1932. Bull. Seism. Soc. Amer. **25** (1935) 62. — 38. B. Gutenberg, The propagation of the longitudinal waves produced by the Long Beach Earthquake. Gerl. Beitr. Geophys. **41** (1934) 114. — 39. I. Lehmann, Transmission times for seismic waves for epicentral distances around 20°. Geodetic Institut København. Meddelelse No. 5 (1934). — 40. C. G. Dahm, New values for dilatational wave velocities through the earth. Transact. Amer. Geophys. Union, 13. annual meeting, Washington **1934**, 80. — Details in his doctorate dissertation, St. Louis University. (Not printed.) — 41. K. Wadati and K. Masuda, On the travel time of earthquake waves. Part VI. The Geophys. Magaz. Tokyo 8 (1934) 187. — 42. B. Gutenberg, Die Geschwindigkeit der Longitudinalwellen im Erdinnern. Gerl. Beitr. Geophys. **17** (1927) 356. — 43. J. A. Fleming, Die siebente Kreuzungsfahrt der Yacht Carnegie. Gerl. Beitr. Geophys. **21** (1928) 345. — 44. H. Jeffreys and K. E. Bullen, Times of transmission of earthquake waves. Publ. Bur. Centr. Séismol. Int. (A) **11** (1935).